AL/EQ-TR-1996-0054

UNITED STATES AIR FORCE
ARMSTRONG LABORATORY

Cationic Surfactant-Enhanced Sorption and Nonionic Surfactant-Enhanced Solubilization of Hydrophobic Organic Contaminants in Groundwater

Joel S, Hayworth, Applied Research Associates, and
David R. Burris, Armstrong Laboratory Environics Directorate

APPLIED RESEARCH ASSOCIATES.
P. O. Box 40128
410 Quakerbridge Road
Tyndall Air Force Base, Florida 32403

April 1997

19981118 109

DTIC QUALITY INSPECTED 4

Environics Directorate
Environmental Risk Management
Division
139 Barnes Drive
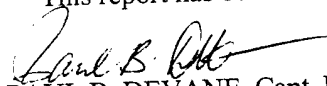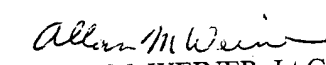Tyndall Air Force Base FL
32403-5323

NOTICES

This report was prepared as an account of work sponsored by an agency of the United States Government. Neither the United States Government nor any agency thereof, nor any employees make any warranty, expressed or implied, or assume any legal liability or responsibility for the accuracy, completeness, or usefulness or any privately owned rights. Reference herein to any specific commercial process, or service by trade name, trademark, manufacturer, or otherwise does not necessarily constitute or imply its endorsement, recommendation, or favoring by the United States Government or any agency, contractor, or subcontractor thereof. The views and opinions of the authors expressed herein do not necessarily state or reflect those of the United States Government or any agency, contractor, or subcontractor thereof.

When Government drawings, specifications, or other data are used for any purpose other than in connection with a definitely Government-related procurement, the United States Government incurs no responsibility or any obligations, whatsoever. The fact that the Government may have formulated or in any way supplies the said drawings, specifications, or other data, is not to be regarded by implication, or otherwise in any manner construed, as licensing the holder or any person or corporation; or as conveying any rights or permission to manufacture, use or sell any patented invention that may in any way be related thereto.

This technical report has been reviewed by the Public Affairs Office (PA) and is releasable to the National Technical Information Service, where it will be available to the general public, including foreign nationals.

This report has been reviewed and is approved for publication.

PAUL B. DEVANE, Capt, USAF, BSC
Project Officer

ALLAN M. WEINER, Lt Col, USAF
Chief, Environmental Risk Management Division

DRAFT SF 298

1. Report Date (dd-mm-yy) April 1997	2. Report Type Final	3. Dates covered (from... to) 1 October 1993 to April 1997	
4. Title & subtitle Cationic Surfactant-Enhanced Sorption and Nonionic Surfactant-Enhanced Solubilization of Hydrophobic Organic Contaminants in Groundwater		5a. Contract or Grant # F08635-93-C-0020	
		5b. Program Element # 62202F	
6. Author(s) Hayworth, Joel S. and David R. Burris		5c. Project # 1900	
		5d. Task #	
		5e. Work Unit # C401	
7. Performing Organization Name & Address Applied Research Associates P.O. Box 40128 Tyndall Air Force Base, FL 32403		8. Performing Organization Report #	
9. Sponsoring/Monitoring Agency Name & Address Armstrong Laboratory Environics Directorate Environmental Risk Management Technologies Division 139 Barnes Drive, Suite 2 Tyndall Air Force Base, FL 32403-5323		10. Monitor Acronym USAF	
		11. Monitor Report # AL/EQ-TR-1996-0054	
12. Distribution/Availability Statement Approved for public release; distribution unlimited.			
13. Supplementary Notes			

14. Abstract   This study was conducted to assess the feasibility of using surfactants to immobilize and recover organic contaminants from groundwater. Before such a remediation method can be employed in the field, a clear understanding of the complex transport, partitioning behavior, and interactions of the surfactants and contaminants in a dynamic groundwater system is required. Batch, column and box aquifer model experiments were conducted to investigate the proposed remediation strategy. Also, numerical modeling tools were developed to predict the coupled cationic/nonionic/HOC transport behavior within a dynamic groundwater system. Experimental results show that it is feasible to create a stationary cationic surfactant-enhanced sorbent zone in situ within an aquifer. The main criteria for sorbent zone development are a relatively high cation exchange capacity, a low carbon content, and a relatively homogeneous and permeable aquifer. Numerical simulation results indicate that mass-transfer limiting desorption of the cationic surfactant will likely occur within an enhanced sorbent zone.   (continued on next page)

15. Subject Terms					

Security Classification of			19. Limitation of Abstract	20. # of Pages	21. Responsible Person (Name and Telephone #)
16. Report Unclassified	17. Abstract Unclassified	18. This Page Unclassified	Unlimited	68	Capt Paul B. Devane (904) 283-6288

14. Continuation from page i:

Experimental results also indicate that nonionic surfactant-enhanced solubilization is extremely efficient in solubilizing and recovering HOCs from within enhanced sorbent zones. However, numerical simulations of the coupled transport of nonionic surfactants and HOCs suggest that mass-transfer limited sorption of the nonionic surfactant will also occur during nonionic surfactant flushing. Based on the probability of mass-transfer limited transport of the surfactants, it is likely that laboratory experiments will be required prior to employing this remediation technique in the field, to determine maximum operating limits on aquifer hydraulics.

PREFACE

This report was prepared by Dr. Joel S. Hayworth (Applied Research Associates, Inc.) and Dr. David R. Burris (Armstrong Laboratory EQL) as an internal final report to the Armstrong Laboratory Environics Directorate.

This report describes a laboratory and numerical modeling study investigating the feasibility of using cationic and nonionic surfactants to immobilize and recover hydrophobic organic contaminants dissolved in groundwater. The results of this study are directly applicable to the design of a cationic surfactant-enhanced sorption/nonionic surfactant-enhanced solubilization groundwater remediation method.

This work was performed as part of the Soil/Surfactant Interactions project. The AL/EQM project officer was Captain Jeffery Stinson, USAF.

(The reverse of this page is blank)

iii

EXECUTIVE SUMMARY

A. OBJECTIVES

The objectives of this study were to investigate the feasibility of using cationic surfactants to create *in situ* enhanced sorbent zones for hydrophobic organic contaminants (HOCs) migrating in groundwater; to couple the sorbent zone concept with scheme to abiotically remove HOCs immobilized within a cationic surfactant-enhanced sorbent zone using a nonionic surfactant flush; and to develop a capability to predict the efficiency of the proposed remediation scheme.

B. BACKGROUND

The release of toxic chemicals into the subsurface environment poses a serious threat to ground water resources. The concept of *in situ* treatment zones has been proposed as a possible alternative approach to pump-and-treat management of groundwater contaminant plumes. Recent laboratory, field, and numerical modeling studies have shown that under certain conditions, surfactants can be used to form stable zones of enhanced sorption for contaminants migrating in groundwater. An aqueous cationic surfactant solution can be injected into an aquifer to create a permeable enhanced sorption zone *in situ*. The *in situ* sorption zone would intercept a migrating HOC plume, retarding the transport of these contaminants. Coupled with a contaminant removal scheme, this concept may prove to be a useful groundwater remediation strategy. One promising removal method involves extracting sorbed contaminants from the sorption zone by enhanced solubilization using an anionic or nonionic surfactant flush. Contaminant-laden surfactant solution could then be removed from the subsurface for treatment above ground.

C. SCOPE

This study was conducted to assess the feasibility of using surfactants to immobilize and recover organic contaminants from groundwater. Before such a remediation method can be employed in the field, a clear understanding of the complex transport, partitioning behavior, and interactions of the surfactants and contaminants in a dynamic groundwater system is required. Batch, column and box aquifer model experiments were conducted to investigate the proposed remediation strategy. Also, numerical modeling tools were developed to predict the coupled cationic/nonionic/HOC transport behavior within a dynamic groundwater system.

E. RESULTS AND CONCLUSIONS

Experimental results show that it is feasible to create a stationary cationic surfactant-enhanced sorbent zone in situ within an aquifer. The main criteria for sorbent zone development are a relatively high cation exchange capacity, a low organic carbon content,

and a relatively homogeneous and permeable aquifer. Numerical simulation results indicate that mass-transfer limiting desorption of the cationic surfactant will likely occur within an enhanced sorbent zone.

Experimental results also indicate that nonionic surfactant-enhanced solubilization is extremely efficient in solubilizing and recovering HOCs from within enhanced sorbent zones. However, numerical simulations of the coupled transport of nonionic surfactants and HOCs suggest that mass-transfer limited sorption of the nonionic surfactant will also occur during nonionic surfactant flushing. Based on the probability of mass-transfer limited transport of the surfactants, it is likely that laboratory experiments will be required prior to employing this remediation technique in the field, to determine maximum operating limits on aquifer hydraulics.

F. RECOMMENDATIONS

Further research investigating this promising remediation strategy is warranted. In particular, laboratory-scale multidimensional physical modeling should be performed to address questions of preferential surfactant distributions in mildly heterogeneous systems. Also, research into surface treatment methods for separating and recovering the nonionic surfactant from the extracted effluent stream is required. Without such recovery methods, it is unlikely that this remediation technique will prove cost-effective. In this regard, an economic analysis of the remediation method should be performed, comparing the method to other established plume remediation techniques (e.g., pump-and-treat) for a hypothetical field site. If such an analysis indicates that the method is cost-effective, then a field-scale demonstration of the method would be appropriate.

TABLE OF CONTENTS

LIST OF FIGURES

(The reverse of this page is blank)

LIST OF TABLES

(The reverse of this page is blank)

SECTION I

INTRODUCTION

A. OBJECTIVES

The objectives of this study were to investigate the feasibility of using cationic surfactants to create *in situ* enhanced sorbent zones for hydrophobic organic contaminants (HOCs) migrating in groundwater; to couple the sorbent zone concept with scheme to abiotically remove HOCs immobilized within a cationic surfactant-enhanced sorbent zone using a nonionic surfactant flush; and to develop a capability to predict the efficiency of the proposed remediation scheme.

B. BACKGROUND

The release of toxic chemicals into the subsurface environment poses a serious threat to groundwater resources. Pools of spilled organic chemicals can be long-term sources of groundwater contamination because they often contain components of low solubility. Most existing plume management schemes depend upon groundwater pump-and-treat technology, which is often a relatively expensive and long-term alternative *(1)*. The concept of *in situ* treatment zones has been proposed as a possible alternative approach to plume management *(2)*.

Recent laboratory, field, and numerical modeling studies have shown that under certain conditions, cationic surfactants can be used to increase the organic carbon content of aquifer materials, forming stable zones of enhanced sorption for HOCs migrating in groundwater *(3-7)*. The process by which this modification takes place is believed to be predominantly cation exchange of the cationic surfactant monomers with the solid phase. An aqueous cationic surfactant solution can be injected into an aquifer to create a permeable enhanced sorption zone *in situ*. The *in situ* sorption zone would intercept a migrating HOC plume, retarding the transport of these contaminants. Coupled with a contaminant removal scheme, this concept may prove to be a useful groundwater remediation strategy *(8)*.

Biodegradation of HOCs within an enhanced sorbent zone is a possible option for the "removal" step of the proposed remediation scheme. However, there is evidence that some cationic surfactants have a toxic effect on HOC-degrading bacteria *(9-11)*. Bioavailability of sorbed HOCs appears to be high for cationic surfactant modified materials due to rapid desorption *(11)*, an encouraging result for biodegradation as the "removal" process. An alternative to biodegradation may be the extraction of HOCs from the sorption zone by enhanced solubilization using an anionic or nonionic surfactant flush.

1

HOC-laden surfactant solution could then be removed from the subsurface for treatment above ground.

The ability of anionic and nonionic surfactants to enhance the solubility of HOCs in an aqueous system is well established *(e.g., 12, 13)*. The mechanism for enhanced solubility is partitioning of HOCs into surfactant micelles. Surfactant micelles form through self-association of surfactant monomers as they reach their critical micelle concentration (CMC). In a soil-water system in which a micelle-forming surfactant is present, enhanced HOC solubility is affected by partitioning of both the surfactant and the HOC to the solid phase. HOC partitioning to the solid phase is essentially governed by the organic carbon content (OC) of the soil, which can be natural and/or enhanced *(5, 14)*.

C. SCOPE

The scope of this study incompassed investigating (1) the transport and partitioning behavior of the cationic surfactant hexadecyltrimethylammonium chloride (HDTMA) in aquifer material collected from a field site at Columbus AFB, MS; (2) the resulting increase in HOC sorption onto the aquifer material resulting from treatment with HDTMA; (3) the transport and partitioning behavior of the nonionic surfactant IGEPAL CO 730 in HDTMA treated and untreated Columbus AFB aquifer material; and (4) the enhanced solubilization of HOCs immobilized within cationic surfactant-enhanced sorbent zones. 1,2,4 trichlorobenzene (TCB) was used during this investigation as a representative HOC. (1) through (4) above were studied using batch, column and box aquifer model experiments. Additionally, the knowledge gained through experimentation was used to develop numerical modeling tools to predict the coupled cationic/nonionic/HOC transport behavior within a dynamic groundwater system. These modeling tools can be used to estimate engineering parameters necessary to employ the enhanced sorption/enhanced solubilization remediation scheme in the field.

SECTION II

CATIONIC SURFACTANT-ENHANCED SORBENT ZONES: EXPERIMENTS

A. METHODOLOGY

1. Aquifer Material

Subsurface material was obtained from the saturated zone at Columbus AFB, Mississippi. The aquifer is an unconfined, fluvial deposit, containing sand and gravel and is described in (15). Approximately 50% of the bulk aquifer material was > 2 mm. The < 2 mm size fraction was used in this study. It contained 90% sand, 2% silt and 8% clay. The cation exchange capacity (CMC) of the < 2 mm material ranged from 2.5 to 2.8 meq/100 g. The organic carbon (OC) content was 0.02%.

2. Chemicals

The following chemicals were used: hexadecyltrimethylammonium chloride (HDTMA; 25% in aqueous solution) from Aldrich Chemical Company; ^{14}C-labeled hexadecyltrimethylammonium iodide (99% radiochemical purity) from American Radiolabeled Chemicals; and $CaSO_4$ and NaN_3 from Aldrich Chemical Company. HDTMA is a quaternary ammonium salt with the chemical formula $CH_3(CH_2)_{15}N(CH_3)_3Cl$. Deionized water and distilled water were used. The water used for all experiments contained 0.005 M $CaSO_4$ (for ionic strength) and 0.02% NaN_3 (to inhibit microbial activity).

3. Sorption Isotherms

The HDTMA on Columbus aquifer material isotherms were determined by the concentration difference method (16). ^{14}C-labeled hexadecyltrimethylammonium iodide was used for the isotherm experiment; solid/liquid phase ratios were chosen to provide sufficient radioactivity in the aqueous phase at equilibrium to minimize potential artifacts due to radiochemical impurities. Centrifuge tubes with Teflon®-lined caps were used. The centrifuge tubes were equilibrated by rotating at 25 °C for 24 hours. The tubes were centrifuged at 2000 rpm for 5 minutes prior to sampling for counting on a Beckman model LS 9800 liquid scintillation counter.

4. Cationic Surfactant Distribution within Columns

Aquifer material was dry-packed into three 25 cm (length) x 2.1 cm (diameter) stainless steel (s.s.) columns (Supelco Company) with 2 µm end frits. To minimize trapped air bubbles, the columns were purged with CO_2, then filled with He-purged water. To each column, 50 mL of 6720 µg/mL HDTMA (as the cation) was added.

3

One was loaded at a flow rate of 0.5 mL/hr and the other two at 50 mL/hr. The columns were then flushed with water (several column pore volumes for the 0.5 mL/hr and one of 50 mL/hr columns; 400 pore volumes for the other 50 mL/hr column). After flushing, the aquifer material was extruded from the column and sectioned for OC analysis.

HDTMA concentrations on the aquifer material were determined using a Leco Model WR-112 Carbon Analyzer. OC determination was suitable for determining HDTMA content because inorganic carbon was negligible, and the OC content of the unmodified Columbus aquifer material was low (~0.02% OC) relative to the increase in OC due to the addition of HDTMA (usually in the 0.2-0.6% OC range), providing a low-level background concentration.

5. Box Model Aquifer Experiment

The box model aquifer used is described in (17). The model was 120 cm (length) x 30 cm (width) x 30 cm (height). The box was constructed from glass sheets joined by RTV Silicone Rubber (Dow Corning). Stainless steel screens of 200 mesh were installed to isolate the aquifer from the head tanks at the ends of the box. A steady average pore water velocity of 15 cm/day was established by maintaining a volumetric flow rate through the box of 2 mL/min.

An injection well (with 2.54 cm vertical screened interval) was used to inject 3.3 L of 1.8% HDTMA along a vertical plane between the third and fourth rows of sampling wells. Injection rates ranged from 1.8 to 4.0 mL/hr, taking place over a 10 day period. The injection well location was periodically moved vertically and horizontally to provide coverage along the injection plane. The HDTMA loading process was monitored by observing the appearance of foam in water obtained from the downgradient sampling wells.

After 3 months of monitoring the progress of the experiment the box was excavated to the well screen depth and sampled for HDTMA distributions. The water table was lowered prior to excavation. Samples for OC analysis were taken throughout the middle plane of the box. Dry sample weight was obtained by subtracting an average water content.

B. RESULTS

The HDTMA sorption isotherm on Columbus soil is shown in Figure 1 (3). It is highly nonlinear with a plateau characteristic of an ion-exchange sorption mechanism. The isotherm plateau corresponds to 2.8 meq HDTMA/100 g, which agrees well with the CEC of the aquifer material (2.5-2.8 meq/100 g). The highly nonlinear nature of the isotherm is important for the *in situ* production of an "essentially immobile" cationic surfactant-modified zone within an aquifer. The movement of the surfactant-modified zone becomes progressively slower as the near vertical region of the isotherm is approached until the zone becomes almost stationary. Interaction of the hydrophobic groups of the surfactant with each other or the aquifer material organic matter may further restrict desorption which would have a positive effect on the sorption zone concept.

The distributions of HDTMA following its addition to aquifer material columns and subsequent flushing with HDTMA-free water are shown in Figure 2. The results show that the sorption reaction is fast since there is no difference between the 0.5 and 50 mL/hr loading rates (with <5 pore volume flushes), which translates to velocities of 8 cm/day and 8 m/day. From a practical standpoint, this indicates that surfactant solution added rapidly to the subsurface should quickly form a sorbent zone. However, a moderate injection rate would be appropriate for heterogeneous aquifers if there is concern that the surfactant will enter lower hydraulic conductivity zones. The 400 pore volume flush caused the HDTMA distribution to spread downgradient, but it still remained in the column. A significant amount of HDTMA (as 18% OC) remained in the sample nearest the column inlet, indicating a significant resistance to transport. There was no detectable column backpressure caused by the addition of the surfactant to the column, suggesting that hydraulic conductivity may not have been significantly reduced. The results also show that this *in situ* method can form an essentially stationary zone of cationic surfactant-modified aquifer material within a flow-through system.

The distribution of HDTMA (as %OC) in the middle horizontal plane of the box model aquifer is shown in Figure 3. The results show that a zone of HDTMA-modified aquifer material was produced in the desired location. The upgradient edge of the zone coincides with the surfactant injection well locations. During the process of injecting the HDTMA solution, there was no increase in the head difference between the inlet and outlet head tanks. Also during the injection process, foam was never observed in water obtained from the third row of sampling wells (i.e., upgradient of the injection well location). These observations indicate that there was no significant decrease in hydraulic conductivity caused by the addition of the surfactant.

5
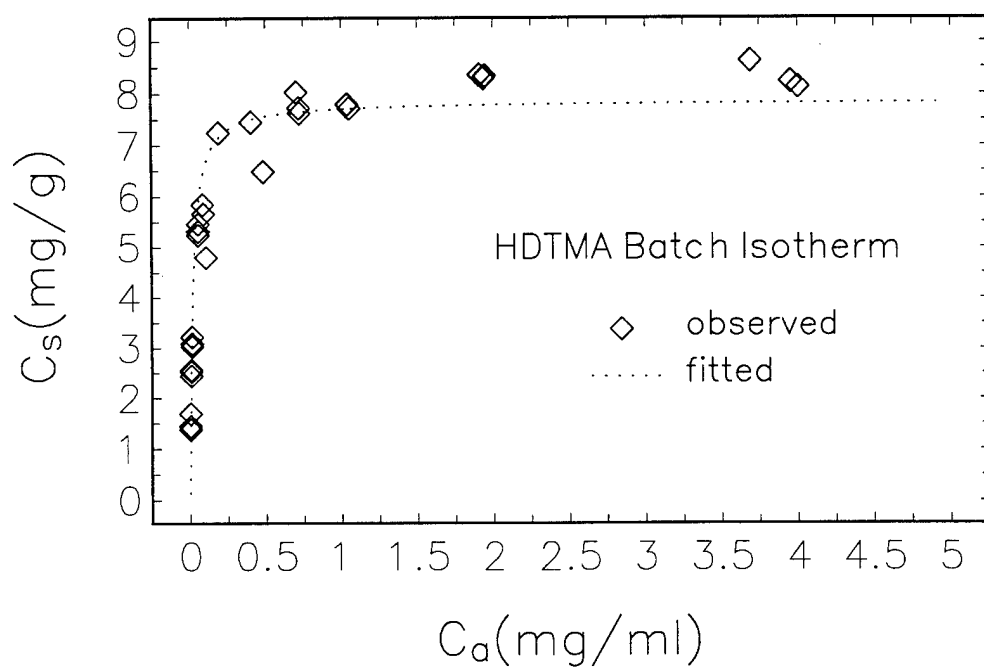
Figure 1. HDTMA batch sorption isotherm for Columbus AFB aquifer material.
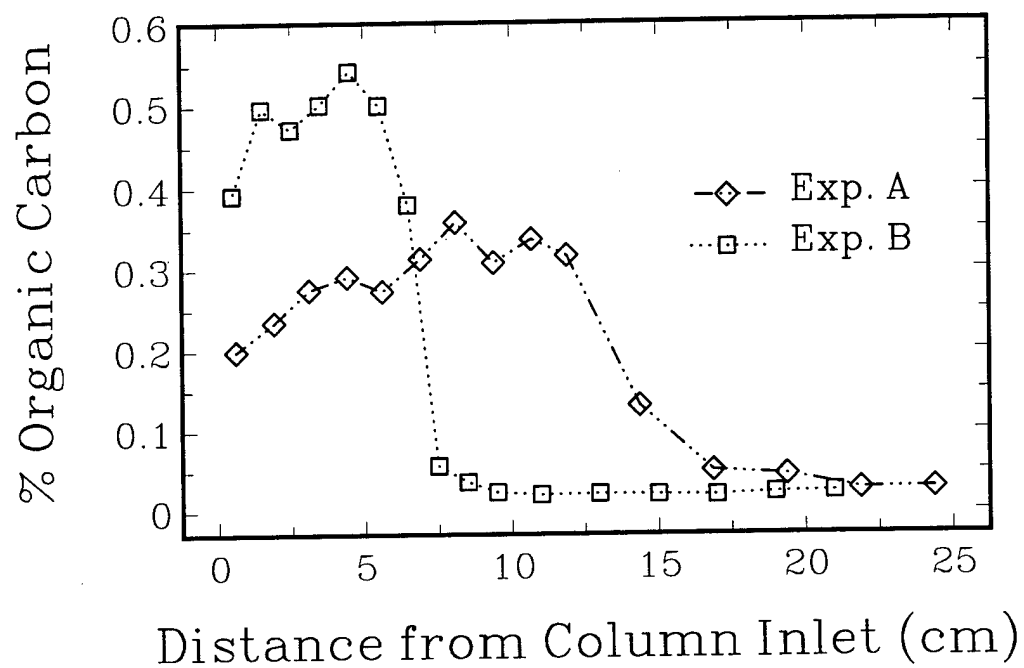
Figure 2. HDTMA (as %OC) distributions on two columns of Columbus AFB aquifer material.
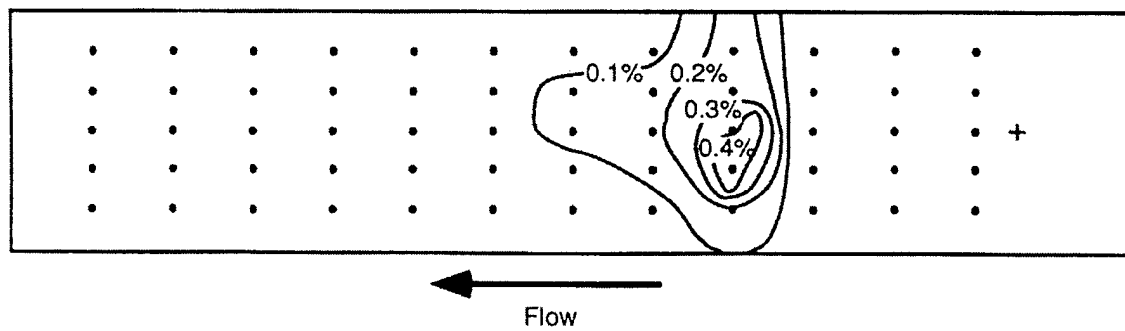
Figure 3.   HDTMA (as %OC) distribution in aquifer box model filled with Columbus AFB aquifer material.

8

SECTION III

CATIONIC SURFACTANT-ENHANCED SORBENT ZONES: SIMULATIONS

A. METHODOLOGY

1. Model Development

The transport of a sorbing contaminant moving with a uniform average horizontal velocity through a fully saturated column packed with a homogeneous porous medium can be described by the one-dimensional advection-dispersion equation:

$$\frac{\partial C_a}{\partial t} + \frac{\rho_b}{\theta}\frac{\partial C_s}{\partial t} = -v\frac{\partial C_a}{\partial x} + D\frac{\partial^2 C_a}{\partial x^2} \tag{1}$$

where x [L_{pm}] and t [T] represent longitudinal position and time, respectively; C_a [$M_a L_a^{-3}$] and C_s [$M_s M_d^{-1}$] are the aqueous- and sorbed-phase concentrations, respectively; ρ_b [$M_d L_{pm}^{-3}$] is the dry bulk density of the medium, θ [$L_a^3 L_{pm}^{-3}$] is the porosity of the medium, v [$L_{pm}T^{-1}$] is the average horizontal pore water velocity, and D [$L_{pm}^2 T^{-1}$] is the longitudinal dispersion coefficient. The subscripts a and s represent the aqueous and sorbed phases, respectively. The subscript pm represents the bulk (saturated) aquifer material, while the subscript d represents the dry aquifer material. If it is assumed that the predominant mixing mechanism is mechanical dispersion, then D in Equation (1) can be approximated by D=αv, where α [L_{pm}] is the longitudinal dispersivity of the porous medium (18).

The HDTMA batch isotherm (Figure 1) has the form of the nonlinear equilibrium Langmuir equation (19), thus it is natural to attempt to model the experimental data using this partitioning relationship:

$$C_s = \frac{kbC_a}{1 + kC_a} \tag{2}$$

In Equation (2), k [$M_a^{-1}L_a^3$] is a constant related to the magnitude of the initial slope of the isotherm, while b [$M_s M_d^{-1}$] represents the value of C_s which is asymptotically approached as C_a increases. For batch partitioning which is controlled by cation exchange, the parameter b is approximately equal to the cation exchange capacity (CEC) of the sorbent; however, in general both k and b should be regarded as empirical constants (19). Differentiating Equation (2) with respect to C_a and substituting the result into Equation (1) gives:

9

$$R\frac{\partial C_a}{\partial t} = -v\frac{\partial C_a}{\partial x} + D\frac{\partial^2 C_a}{\partial x^2} \tag{3}$$

where R is the nonlinear, equilibrium Langmuir retardation coefficient:

$$R = R(C_a) = 1 + \frac{\rho_b}{\theta}\frac{kb}{(1+kC_a)^2} \tag{4}$$

Because of the likelihood of kinetic effects, a nonequilibrium form of the Langmuir equation was also utilized (20):

$$\frac{\partial C_s}{\partial t} = k_f C_a (b-C_s) - k_b C_s \tag{5}$$

where k_f $[M_a^{-1}L_a^3 T^{-1}]$ and k_b $[T^{-1}]$ are the kinetic Langmuir forward (sorption) and reverse (desorption) reaction rate constants, respectively. Equation (5) describes sorption which is second-order in the forward direction, and first-order in the reverse direction. When the time derivative is equal to zero (i.e., equilibrium conditions), Equation (5) reduces to Equation (2), with $k=k_f/k_b$. Substituting Equation (5) into Equation (1) gives the nonlinear, kinetic Langmuir transport equation:

$$\frac{\partial C_a}{\partial t} = -v\frac{\partial C_a}{\partial x} + D\frac{\partial^2 C_a}{\partial x^2} - \frac{\rho_b}{\theta}\left[k_f C_a(b-C_s) - k_b C_s\right] \tag{6}$$

Previous researchers (21) found in batch experiments that hydrophobic sorption of cationic surfactants to alumina and silica substrates could be represented by a modified form of the Brunauer-Emmett-Teller (BET) equation (22):

$$C_s = \frac{k_c b X}{(1-X)}\frac{1-(n+1)X^n+nX^{n+1}}{1+(k_c-1)X-k_c X^{n+1}} \tag{7}$$

where n (an integer) is the number of sorbed layers, k_c is a dimensionless constant related to the magnitude of the initial slope of the batch isotherm, C_M $[M_a L_a^{-3}]$ is the CMC, and $X=C_a/C_M$. The constant b represents the sorbed concentration when complete monolayer coverage is achieved; however, as in the case of Langmuir partitioning, k_c and b should be considered as empirical constants. It should be emphasized that Equation (7) is only valid for aqueous concentrations below the CMC. For sorption described by Equation (7), the value of C_a corresponding to saturation of the sorption sites on the solid surface will be less than the CMC. Above this value of C_a, multi-layer, secondary sorption will occur until $C_a \approx$ CMC. For values of C_a above the CMC, aqueous surfactant molecules will be incorporated into micelles; thus,

10

maximum sorption occurs when $C_a \approx CMC$. When n=1, Equation (7) reduces to Equation (2) with $k_c = C_M k$. The equilibrium retardation equation (Equation (3)) is also valid for partitioning described by Equation (7), where now R is given by:

$$R(C_a) = 1 + \frac{\rho_b}{\theta} \frac{k_c b}{C_M} \frac{\gamma \eta' - \eta \gamma'}{\gamma^2} \tag{8a}$$

where:

$$\gamma = 1 + (k_c - 2)X - (k_c - 1)X^2 - k_c X^{n+1} + k_c X^{n+2} \tag{8b}$$

$$\gamma' = (k_c - 2) - 2X(k_c - 1) - (n+1)k_c X^n + (n+2)k_c X^{n+1} \tag{8c}$$

$$\eta = X - (n+1)X^{n+1} + nX^{n+2} \tag{8d}$$

$$\eta' = 1 - (n+1)^2 X^n + (n^2 + 2n)X^{n+1} \tag{8e}$$

By comparison with Equations (2), (5) and (7) a first-order, reversible nonlinear kinetic equation can be written:

$$\frac{\partial C_s}{\partial t} = \frac{k_{cf} b X}{(1-X)} \frac{1 - (n+1)X^n + nX^{n+1}}{1 + (k_c - 1)X - k_c X^{n+1}} - k_{cb} C_s \tag{9}$$

k_{cf} [T^{-1}] and k_{cb} [T^{-1}] are the kinetic modified BET forward (sorption) and reverse (desorption) reaction rate constants, respectively. When the time derivative is equal to zero, Equation (9) reduces to Equation (7), with $k_c = k_{cf}/k_{cb}$. Equation (9) can be substituted into Equation (1) to give the nonlinear, nonequilibrium modified BET transport equation:

$$\frac{\partial C_a}{\partial t} = -v \frac{\partial C_a}{\partial x} + D \frac{\partial^2 C_a}{\partial x^2} - \frac{\rho_b}{\theta} \left[k_{cf} b \frac{\eta(C_a)}{\gamma(C_a)} - k_{cb} C_s \right] \tag{10}$$

2. Numerical Method

The finite-difference, Crank-Nicholson numerical technique was used to solve the equilibrium (Equations (3), (4), and (8)) and kinetic (Equations (5), (6), (9) and (10)) Langmuir and modified BET transport equations. This method was chosen because of its relatively straightforward formulation, and because of the simple geometry of the problem. Nonlinearities in the partial differential equations were handled numerically using a Picard iterative scheme (23). The above equations were solved subject to a continuous mass-flux inflow boundary condition, and a continuous aqueous concentration outflow boundary condition. Initially, both the aqueous phase and sorbed phase concentrations throughout the column were equal to zero. Numerical dispersion and numerical oscillations were controlled by discretizing the problem so that the grid Peclet and Courant number criteria were satisfied (24).

Formulating the boundary conditions as described above will lead to conservation of mass. Because there are no analytical solutions to compare with the numerical solutions determined from the model, the numerical accuracy of the model output was evaluated based mainly on mass balance considerations. An exception to this was in the simulations using equilibrium Langmuir sorption, for which comparisons with the computer model MOC (25) were also performed, with good agreement. Mass-balance calculations were made by equating the total mass flux through the column to the total mass stored within the column at a given time. Mass-balance was considered satisfactory when the relative difference between the total mass flux through the column and the total stored mass was below 2%, however in most simulations this difference was below 0.3%.

3. Model Parameters

The isotherm in Figure 1 is characterized by nonlinear, Langmuir-type sorption (19). The column distributions of HDTMA shown in Figure 2 constitute the available data for direct comparison with numerical simulation results. In these experiments, a pulse of HDTMA solution was introduced into a column filled with aquifer material and saturated with simulated ground water, at a constant volumetric loading rate, Q_L. This pulse was followed by a period of flushing with clean pore water at a constant volumetric flushing rate, Q_F. At the end of an experiment, the column was extruded and sectioned for organic carbon analysis. Organic carbon analysis provided a direct estimate of the sorbed HDTMA concentration, because the natural organic carbon content was relatively low compared to the increase in organic carbon due to addition of HDTMA (~0.02 % OC versus 0.2-0.6 % OC), and because the inorganic carbon content was undetectable. The extrusion process reduced the length of the column of aquifer material from 25 cm to approximately 22 cm. This translates to a maximum relative error in the longitudinal position of the observed data of approximately 12%. Unfortunately, it is not known how the positioning error was distributed along the length of the column, so it is not possible to correct for this error in a quantitative way.

However, it should be kept in mind when considering differences between experimental and simulation results. Conditions used in the two column experiments, with large and small flushing rates, are summarized in Table 1.

The column-scale longitudinal dispersivity of the aquifer material (α=0.92 cm) was estimated using tritiated water breakthrough curves from (3). Model parameters for the equilibrium simulations followed directly from the batch sorption data. For the nonequilibrium simulations, estimates of the sorption and desorption mass-transfer terms were obtained by fitting the model to the experimental column data given in Figure 2, using the Levenberg-Marquardt (LM) nonlinear parameter estimation method (26). The methods used to obtain the required model parameters are discussed below, and these parameters are summarized in Table 1.

Table 1. Experimental Conditions for HDTMA Column Studies

	Exp. A	Exp. B
Source concentration[a] (C_o)	6.72 mg/ml	6.72 mg/ml
Volume of source fluid added (V_L)	50 ml	50 ml
Volumetric loading rate (Q_L)	60 ml/hr	50 ml/hr
Total mass HDTMA added	336 mg	336 mg
Loading time	0.83 hr	1.01 hr
Volumetric flushing rate	60 ml/hr	6.0 ml/hr
Flushing time	242.6 hr	66.7 hr
Total column pore volumes flushed	389	12.6

[a] Concentration as the cation

a. Equilibrium Langmuir Partitioning

The batch sorption data shown in Figure 1 can be linearized by plotting the distribution coefficient, K_d, versus C_s:

$$K_d = -kC_s + bk \tag{11}$$

where $K_d=C_s/C_a$, yielding the equilibrium Langmuir coefficients k and b (53 ml/mg and 7.85 mg/g, respectively) defined in Equation (2). The value for b is within the

13

measured range for CEC (2.5-2.8 meq/100 g, or 7.1-7.9 mg/g) for the Columbus aquifer material.

b. Kinetic Langmuir Partitioning

Initial values for k_f and k_b were determined by noting that, for small values of C_a, Equation (2) can be written as $C_s \approx k b C_a$. If it is assumed that the forward (sorption) reaction is "fast," then the ratio k_f/k_b can be approximated by kb. This assumption was based on previous studies by researchers investigating the behavior of cationic surfactants on soil surfaces (27, 28). Thus, when fitting the kinetic Langmuir model, k_f/k_b was held constant at 416 ml/mg, and k_b was varied from an initial (arbitrary) value of 0.1 hr^{-1} until the best fit to the experimental data was obtained, with $k_f=(416$ ml/mg)(k_b). Conditions for Exp. A were used to determine k_f and k_b (268 ml/mg hr and 0.643 hr^{-1}, respectively), and these values were then used to simulate the column distribution for Exp. B.

c. Equilibrium Modified BET Partitioning

For C_a < CMC and n>1, Equation (7) can be approximated by:

$$C_s = \frac{k_c b C_a}{(C_M - C_a)\left[1 + (k_c - 1)\dfrac{C_a}{C_M}\right]} \tag{12}$$

which can be written as a linear equation:

$$\frac{C_a}{C_s(C_M - C_a)} = \frac{k_c - 1}{k_c b}\frac{C_a}{C_M} + \frac{1}{k_c b} \tag{13}$$

By plotting the low concentration batch data according to Equation (13), values for k_c (52.4) and b (4.54 mg/g) were determined, using a value for C_M of 0.32 mg/ml graphically estimated from the batch sorption data (29). These values for k_c and b were then substituted into Equation (7), which was subsequently fit to the batch isotherm to determine the best value for the parameter n (n=2).

d. Kinetic Modified BET Partitioning

The value for C_M and b were the same as those used in the equilibrium modified BET simulations (0.32 mg/ml and 4.54 mg/g, respectively). The forward and reverse mass-transfer terms, k_{cf} and k_{cb}, and the number of sorbed layers, n, (486 hr^{-1}, 0.654 hr^{-1}, and 2, respectively) were determined by fitting the model to the HDTMA column distribution data from Exp. A, using the LM nonlinear parameter estimation method. Initial values for the mass-transfer terms were determined in

14

a manner similar to that employed for kinetic Langmuir partitioning, by noting that for small values of C_a, Equation (12) can be written as $C_s \approx (k_c b/C_M)C_a$. Under the assumption of "fast" sorption, k_{cf}/k_{cb} can be approximated by $k_c b/C_M$. Therefore, when fitting the kinetic modified BET model, k_{cf}/k_{cb} was held constant at 743 ml/g, and k_{cb} was varied from an initial (arbitrary) value of 0.3 hr^{-1} until the best fit to the experimental data was obtained, with $k_{cf}=(743\ ml/g)(k_{cb})$.

B. RESULTS

Simulation results for experiments A and B, using the equilibrium and kinetic Langmuir partitioning relationships, are shown in Figures 4a and 4b, respectively. Figure 4a strongly suggests that during Exp. A, local equilibrium was not attained. For kinetic Langmuir partitioning, the assumption which governed the choice of forward and reverse mass-transfer terms, namely that sorption is fast and desorption is the rate-limiting mechanism controlling the distribution of HDTMA, provided a reasonable fit to the observed distribution. Similar conclusions can be reached concerning Exp. B (Figure 4b), although in this experiment the difference between equilibrium and nonequilibrium partitioning is less pronounced. It should be emphasized that the forward and reverse mass-transfer terms used in the kinetic Langmuir simulation of Exp. B were determined by fitting the model to the data from Exp. A. Parameter fitting directly to the data from Exp. B produced similar results.

Differences between equilibrium and nonequilibrium partitioning for simulations of experiments A and B can likely be attributed to the high pore water velocity during flushing in Exp. A (40.1 cm/hr) relative to Exp. B (4.3 cm/hr), a conclusion which is supported in the literature (30, 31). At higher pore water velocities, there is insufficient time for equilibrium to be established between the aqueous and sorbed phase, thus kinetic effects dominate. As the pore water velocity decreases, conditions more favorable to equilibrium partitioning can develop. In terms of application of the enhanced sorption zone concept in a field situation, natural pore water velocities at the Columbus, MS site in excess of that used in Exp. B have been observed (15). Additionally, when developing an enhanced sorption zone, significant increases in near-field pore water velocities would be expected during surfactant injection and subsequent flushing. Thus, the expectation of kinetic effects during sorption zone development under field conditions is not unreasonable.

The fundamental question as to whether or not the assumption of local equilibrium is valid depends on a number of factors, such as the transport system dynamics (pore water velocity, dispersion coefficients, boundary conditions) as well as the other system parameters and the assumed form of the kinetic partitioning relationship (30). For the simulations performed in this study, it is clear that pore water velocity influenced the final sorbed distribution of HDTMA. It is difficult to assess the overall validity of our choice of kinetic relationships, since the mass-transfer terms were
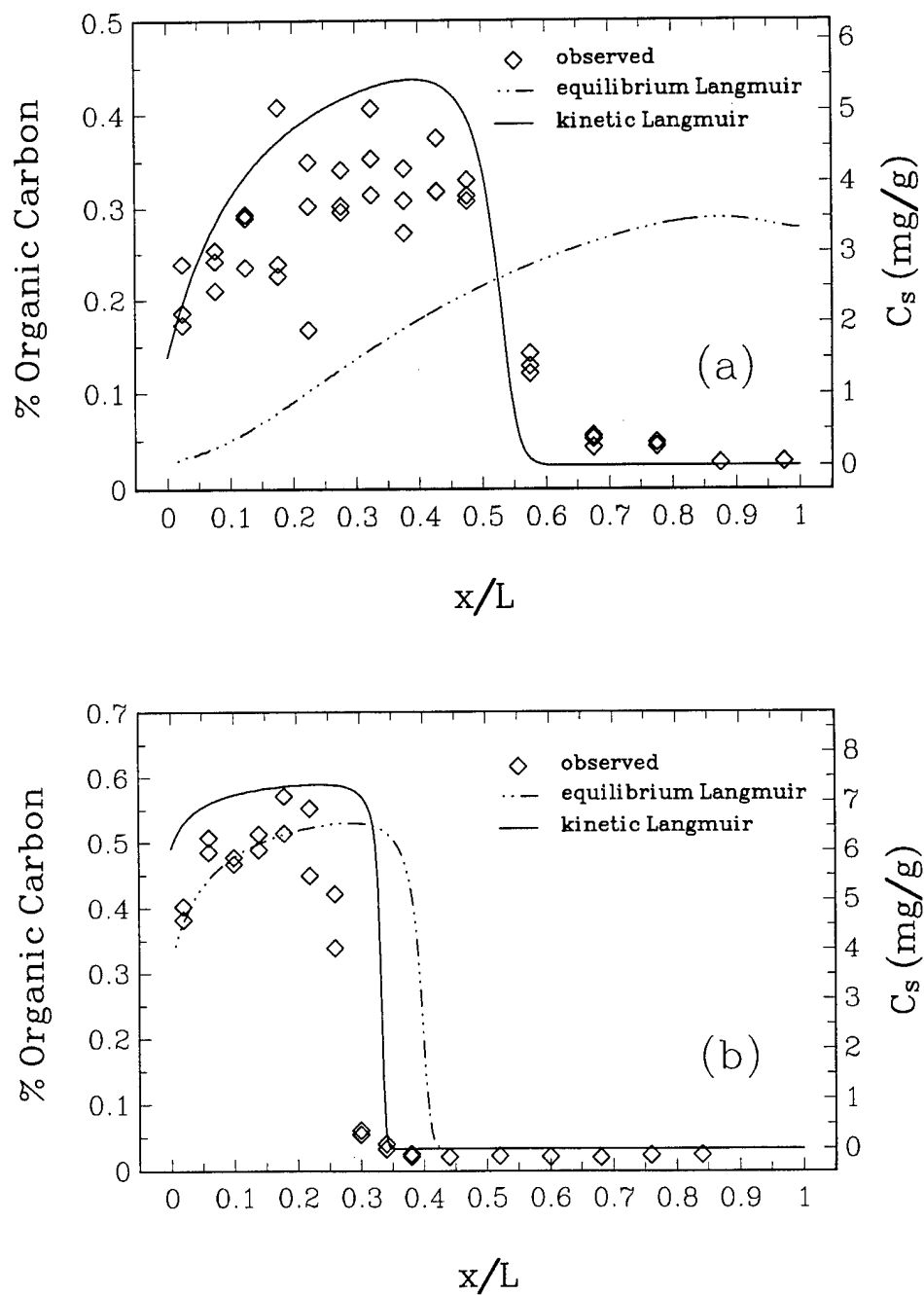
15

Figure 4. Observed and simulated organic carbon distributions (as % OC and C_s) on column of Columbus, MS aquifer material, (a) conditions for Exp. A, and (b) conditions for Exp. B. Simulated distributions obtained using equilibrium and kinetic partitioning.

obtained using estimation methods. Nevertheless, it is reasonable to conclude that kinetic partitioning did occur during these experiments.

Simulation results for Exp. A, using the equilibrium and kinetic modified BET partitioning relationships, are shown in Figure 5. These results further support the conclusion that local equilibrium was not attained during this experiment. The simulated HDTMA distribution using the kinetic modified BET relationship represents the observed distribution well, although the predicted distribution front extends farther down the column than the observed distribution front. However, this apparent discrepancy may be less pronounced when the error in the longitudinal position of the observed data is considered. In light of this, comparison of Figure 5 with Figure 4a indicates that either the kinetic Langmuir or the kinetic modified BET relationship can be used to simulate cationic surfactant transport. From a practical modeling standpoint, the kinetic Langmuir relationship may be the most useful of the two, because it is significantly easier to incorporate into a transport model, and requires one less parameter than the modified BET relationship.

HDTMA breakthrough curves at 5 cm from the column inlet (x/L=0.2) for Exp. A, simulated with the equilibrium and kinetic Langmuir partitioning relationships, are shown in Figures 6a and 6b. Similar figures were obtained for Exp. B using the Langmuir partitioning relationships, as well as experiments A and B using the modified BET relationships. In Figures 6a and 6b, normalized phase concentration is plotted as a function of column pore volumes flushed (dimensionless time, vt/L). For the aqueous phase, $C_\xi=C_a$ and $C_N=C_o$, while for the sorbed phase, $C_\xi=C_s$ and $C_N=kbC_o/(1+kC_o)$, with $k=k_f/k_b$ for kinetic Langmuir partitioning. For the latter case, C_N represents the theoretical maximum sorbed-phase concentration. In Figure 6a, the initial breakthrough after flushing with three column pore volumes is shown, while Figure 6b shows the entire breakthrough over 389 column pore volumes. As Figure 6a illustrates, the aqueous-phase breakthrough for both equilibrium and kinetic partitioning is highly nonlinear, which is expected considering the relatively high source concentration (see Equation (2)). Initial breakthrough for both phases occurs at essentially the same time for both kinetic and equilibrium partitioning, which follows from the assumption of fast sorption and the choice of the forward mass-transfer term, k_f.

The influence of slow desorption on the distribution of HDTMA is illustrated in Figure 6b. The rate of desorption predicted using the kinetic Langmuir relationship is significantly smaller than that predicted using the equilibrium Langmuir relationship. Comparing Figure 6a with Figure 6b, it is apparent that the final sorbed distribution of HDTMA is weakly dependent on the sorption mass-transfer step; rather, this distribution is essentially controlled by the rate of HDTMA desorption. In this regard, the possibility of rate-limiting desorption is supported by recent laboratory studies.
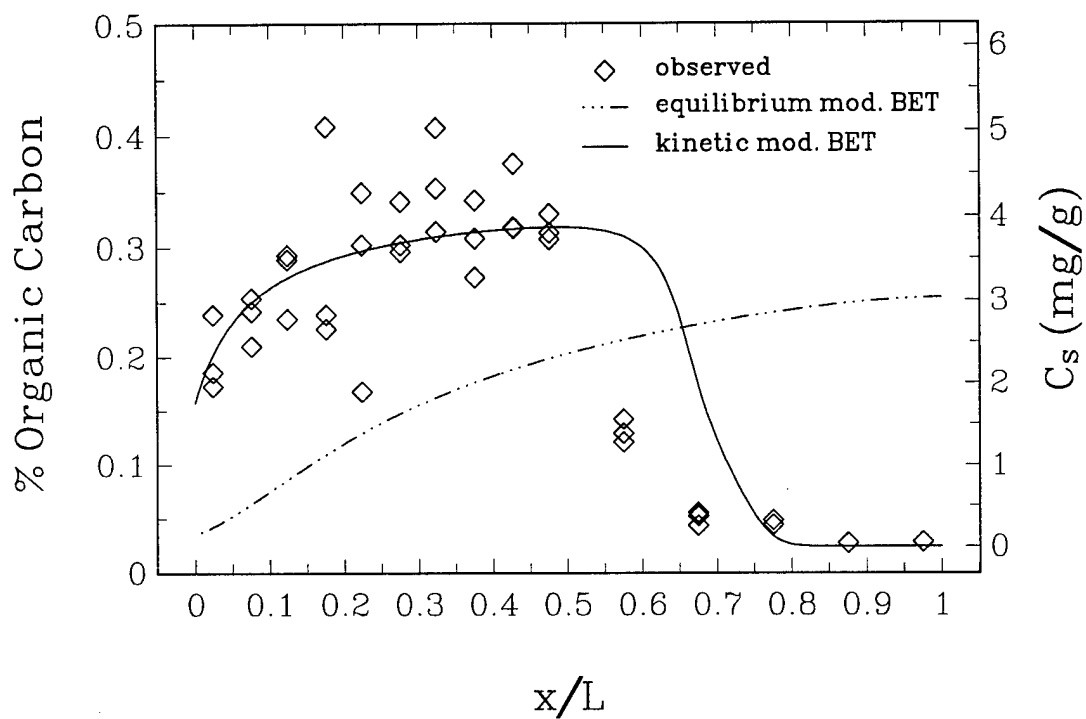
Figure 5.   Observed and simulated organic carbon distributions (as % OC and C_s) on column of Columbus, MS aquifer material, using conditions for Exp. A. Simulated distributions obtained using equilibrium and kinetic modified BET partitioning.
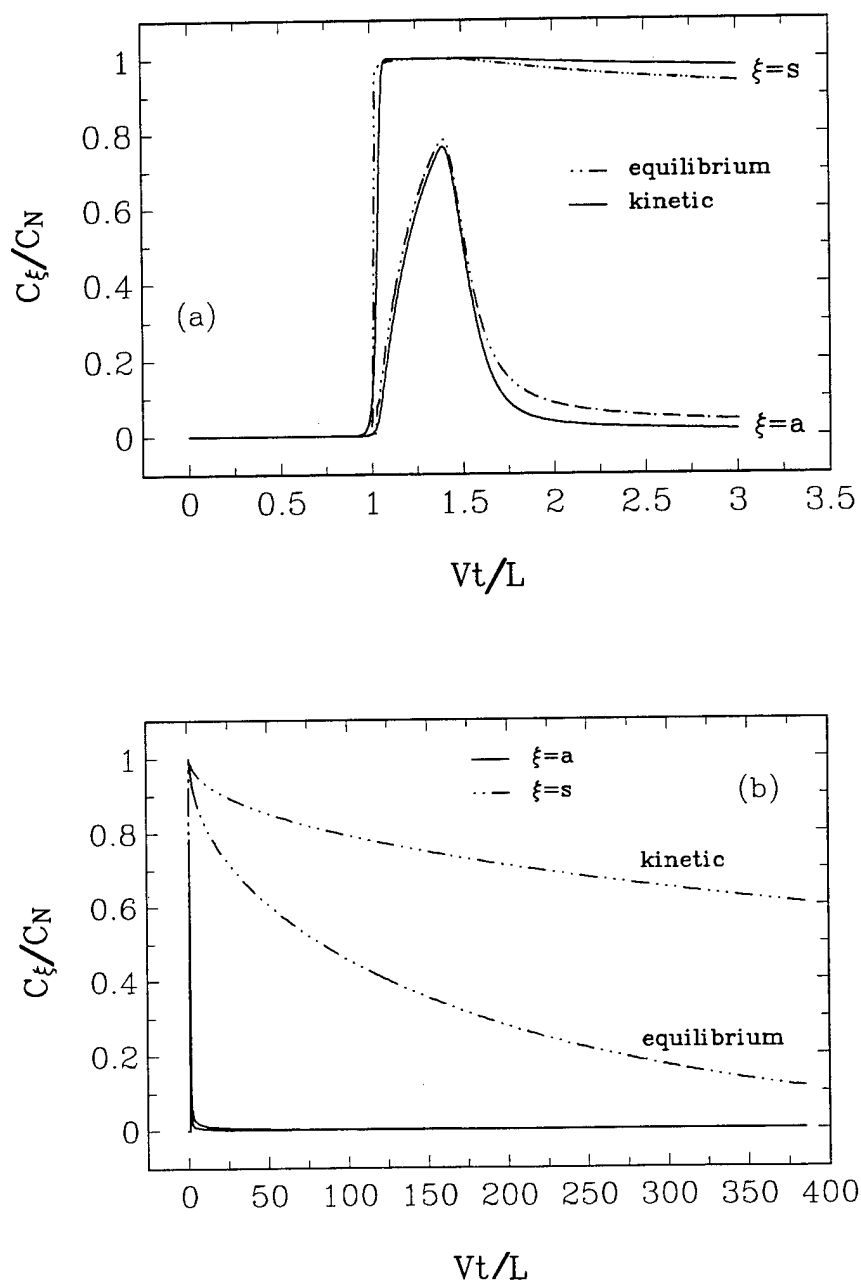
Figure 6. Simulated sorbed and aqueous HDTMA breakthrough for conditions of Exp. A, 5 cm from the column inlet, (a) after flushing with three pore volumes, and (b) after flushing with 389 pore volumes. Simulations obtained using equilibrium and kinetic Langmuir partitioning.

19

Previous researchers *(27)* observed during batch experiments with DP and Lula aquifer material that the distribution coefficient (K_d) determined after a one hour desorption experiment was 21% greater than the K_d determined after a one hour sorption experiment, under otherwise comparable conditions. This suggests that desorption occurred at a slower rate than sorption. Also, recent batch experimental studies *(28)* investigating the stability of cationic surfactant-modified clays (oregano-clays) found that soils which have a significant clay fraction can exhibit desorption hysteresis.

Considering Figures 6a and 6b in the context of Figures 4a, 4b and 5, the assumption of fast sorption/slow desorption provides a reasonable fit to the observed sorbed-phase HDTMA distribution. Nevertheless, because of the relatively high pore water velocities used during these experiments, it is possible that mass transfer resistance during sorption also existed. This possibility is further evidenced by differences in the sorbed phase distributions predicted by the two kinetic relationships, which are directly related to the representation of the sorption mass-transfer step in these models, since the desorption step is first-order and linear for both models. This implies that the assumption of fast sorption/slow desorption may not be entirely correct. The possibility of slow sorption in addition to slow desorption was investigated by examining the sensitivity of the kinetic Langmuir model to the sorption/desorption ratio (k_f/k_b), using the results of Exp. A (Figure 7). An examination of the sensitivity of the kinetic modified BET model to k_{cf}/k_{cb} produced similar results. Each simulation shown in Figure 7 was obtained by holding k_f/k_b at a particular constant value while varying k_b until the best fit was obtained, using the LM parameter estimation method. Decreasing k_f/k_b resulted in a concomitant reduction in k_f below the equilibrium rate, which in turn provided a better fit to the observed sorbed-phase distribution. Aqueous-phase breakthrough curves (similar to Figure 6a) for these simulations are shown in Figure 8. As this figure shows, the peak aqueous-phase breakthrough for each simulation occurs at approximately the same time, suggesting that the average retardation is only slightly dependent on the rate of sorption. However, the initial breakthrough for both phases occurs earlier, and the maximum breakthrough concentrations are lower, as the rate of sorption decreases. Thus, mass-transfer resistance in the sorption reaction results in an increase in the dispersion of the aqueous phase. This has been noted by other researchers utilizing kinetic partitioning relationships to study solute transport in porous media *(32, 33)*, and by researchers studying cationic surfactant transport in the laboratory *(4)*. In the experiments simulated in the present work, it is possible that mass-transfer resistance occurs in both the forward and the reverse reactions, although it is not possible to state this conclusively. Regardless, it is likely that slow desorption is the dominant controlling influence on HDTMA distribution.

One result of the slow desorption of HDTMA illustrated in Figure 6b is the persistence of a background aqueous HDTMA concentration, as shown in Figure 9. In this figure, the aqueous HDTMA concentration predicted to remain at 5 cm from the column inlet

20
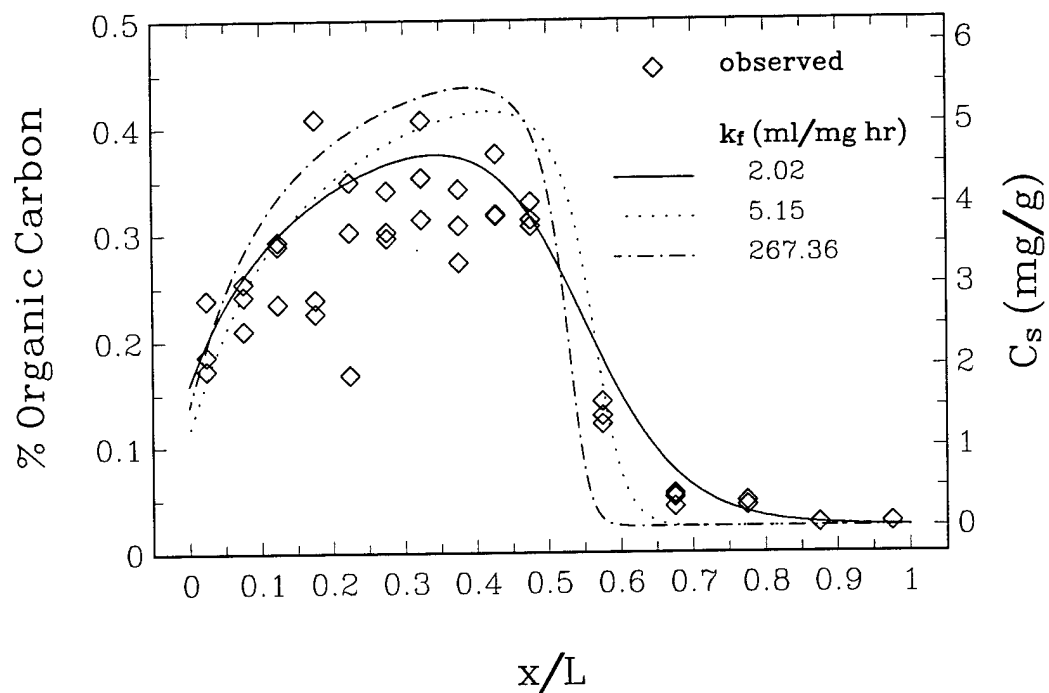
Figure 7. Sensitivity of simulated organic carbon distributions (as % OC and C_s) to the rate of sorption for kinetic Langmuir partitioning. Simulated distributions obtained using conditions for Exp. A.
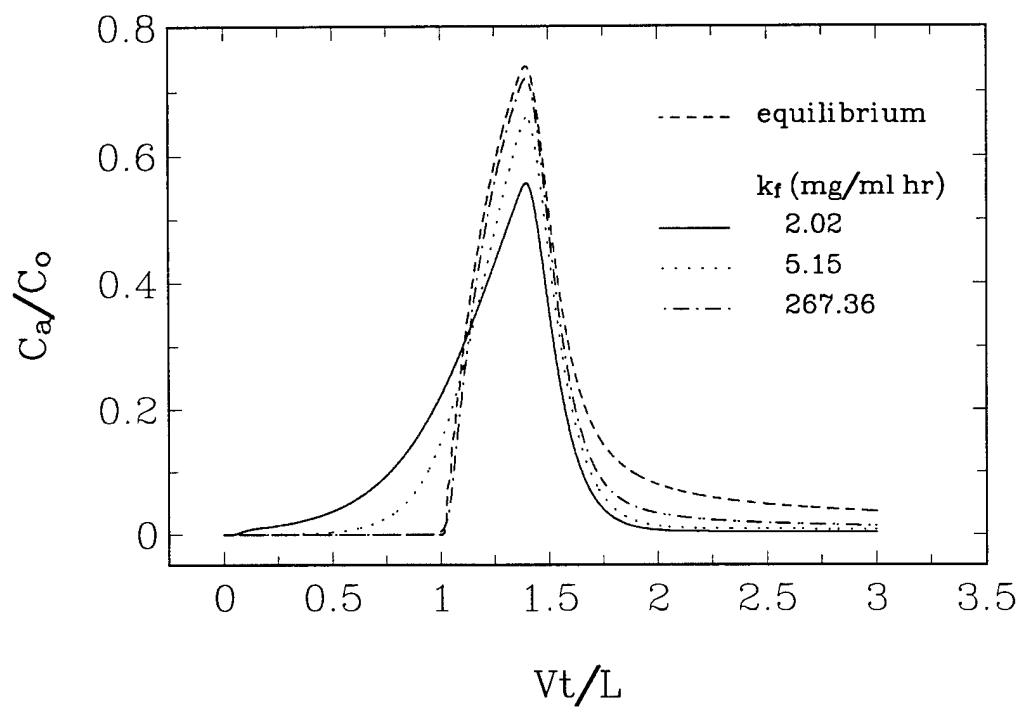
Figure 8. Simulated dimensionless aqueous phase breakthrough at 5 cm from the column inlet, after flushing with three column pore volumes. Simulations obtained using kinetic Langmuir partitioning and conditions of Exp. A, and varying the rate of sorption.

22
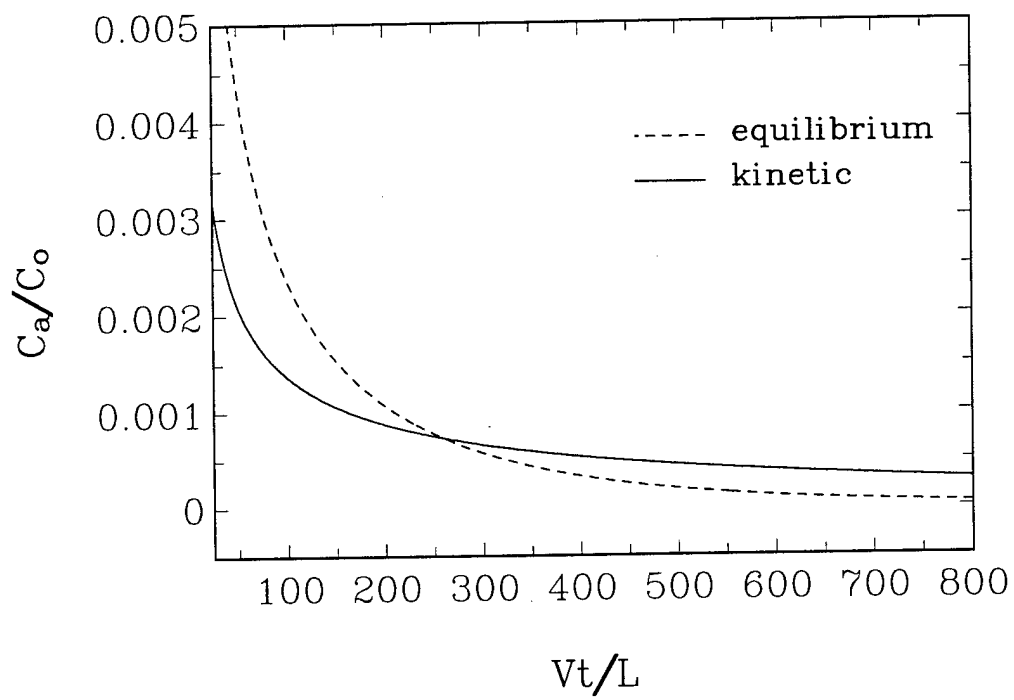
Figure 9. Simulated dimensionless aqueous phase concentration at 5 cm from the column inlet, after flushing with 800 column pore volumes. Simulations obtained using equilibrium and kinetic Langmuir partitioning.

after an extended period of flushing is shown, using equilibrium and kinetic Langmuir partitioning. Although the aqueous concentration in Figure 9 is plotted as thedimensionless parameter C_a/C_o, it is important to note that the background aqueous concentration (C_a) is in fact independent of the source concentration, assuming that initially, maximum sorption was achieved. This results from the fact that desorption will control the aqueous concentration following sufficient flushing to remove the initial high concentration HDTMA pulse. Thus, the range of the background concentration predicted using kinetic Langmuir partitioning (approximately 7-3 ppm HDTMA) shown in Figure 9 represents the anticipated maximum background aqueous HDTMA concentration after flushing with approximately 100 column pore volumes.

Creating a cationic surfactant-enhanced sorbent zone within a natural aquifer will likely require injecting a surfactant solution with a concentration significantly greater than the CMC. The high surfactant concentration within the bulk injected fluid would greatly decrease the amount of time required to form the sorbent zone; however, the large initial aqueous surfactant concentration may act to reduce the size of the microbial community. This in fact has been observed in the laboratory (34); this study found that initially high aqueous concentrations of HDTMA exerted an adverse impact on aerobic heterotrophic HOC-degrading bacteria. However, once the HDTMA became bound to the solid surface, its toxicity to these soil microbes was greatly reduced. Toxicity studies using aquatic microbes have shown that chronic exposure to some cationic surfactants in the concentration range of 0.001 to 10 ppm resulted in an adaptive response, and a significant increase in the number and activity of viable HOC-degrading bacteria (35). This is in the range of the background aqueous concentration predicted in Figure 9, and suggests that if some microbes survive an initial cationic surfactant pulse, they potentially can adapt and recolonize, and therefore be available for degrading subsequently sorbed HOCs. Regardless, once a sorption zone has been established, it is reasonable to expect that "reinoculation" of this zone by HOC-degrading bacteria would occur as a result of migration via ambient ground water flow.

It is important to emphasize the approximate nature of the partitioning relationships used in this study. The assumptions which justify these relationships are discussed in detail in the literature (e.g., 36, 37). Of particular relevance to this study is that for Langmuir partitioning, hydrophobic sorption is not explicitly accounted for, while for modified BET partitioning, multilayer sorption is idealized in ways which simplify this phenomenon considerably. Also, both partitioning relationships assume that adjacent molecules within a sorbed layer do not interact with one another, whereas it is more likely that these interactions will be of comparable magnitude to those due to hydrophobic bonding (37). Thus, although modified BET partitioning is intuitively more attractive than Langmuir partitioning, both require simplifying assumptions which differ from reality. It is possible to develop a more realistic model which would explicitly account for the differences in sorptive behavior between cationically-bound and hydrophobically-bound surfactant monomers, as well as intra-layer effects; however,

24

such a model would require many additional (and difficult to determine) mass-transfer terms, and it is questionable whether the final result would be much improved from that provided by the kinetic Langmuir and kinetic modified BET relationships.

SECTION IV

NONIONIC SURFACTANT-ENHANCED SOLUBILIZATION OF HOCs FROM WITHIN CATIONIC SURFACTANT-ENHANCED SORBENT ZONES: EXPERIMENTS

A. METHODOLOGY

1. Theory

Figure 10 shows a conceptual representation of the partitioning behavior of an HOC, a micelle-forming nonionic surfactant, and a micelle-forming cationic surfactant in a soil-water system. The terms "soil" and "aquifer material" will be used interchangeably in this report. The bulk aqueous phase can be conceptually subdivided into three parts: surfactant-free aqueous phase, surfactant monomer pseudophase and surfactant micellar pseudophase. K^* $[L_a^3 M_{pm}^{-1}]$ is the apparent partitioning coefficient for the HOC between the bulk aqueous phase and the solid phase; K_{MN} $[L_a^3 M_{MN}^{-1}]$ is the HOC partitioning coefficient between the surfactant monomer pseudophase and the bulk aqueous phase; K_{MC} $[L_a^3 M_{MC}^{-1}]$ is the HOC partitioning coefficient between the surfactant micellar pseudophase and the bulk aqueous phase; K_{NS} $[L_a^3 M_{pm}^{-1}]$ represents partitioning of the nonionic surfactant between the bulk aqueous and solid phases, and K_{CS} $[L_a^3 M_{pm}^{-1}]$ represents partitioning of the cationic surfactant between the bulk aqueous and solid phases. The subscripts MN and MC represent surfactant monomers and micelles; the subscripts NS and CS represent the nonionic and cationic surfactants, respectively. The subscripts a and pm represent the bulk aqueous phase and the bulk (saturated) porous medium, respectively.

In the system described by Figure 10, HOC partitioning is dependent on the aqueous surfactant concentration (nonionic and cationic) and the organic carbon content of the soil. Following previous studies on soil systems with nonionic surfactants alone (e.g., 13, 39), K^* can be written as:

$$K^* = K_d \frac{(1 + \kappa_{OC,NS} X_{OC,NS})}{(1 + K_{MN} C_{MN,a} + K_{MC} C_{MC,a})} \qquad (14)$$

where K_d $[L_a^3 M_{pm}^{-1}]$ is the soil-water distribution coefficient for the HOC; $X_{OC,NS}$ $[M_{NS} M_{OC}^{-1}]$ represents the sorbed nonionic surfactant mass per unit mass of soil organic carbon (OC); κ_{OC} $[M_{OC} M_{NS}^{-1}]$ is the partitioning coefficient for the HOC between the sorbed nonionic surfactant and the soil organic carbon; and $C_{MN,a}$ and $C_{MC,a}$ are the aqueous concentrations of the nonionic surfactant monomers and micelles, respectively. The use of volumetric concentrations ($C_{MN,a}$ and $C_{MC,a}$) differs from earlier studies (13, 39) and results in dimensional K_{MN} and K_{MC} values; however, it is an advantageous
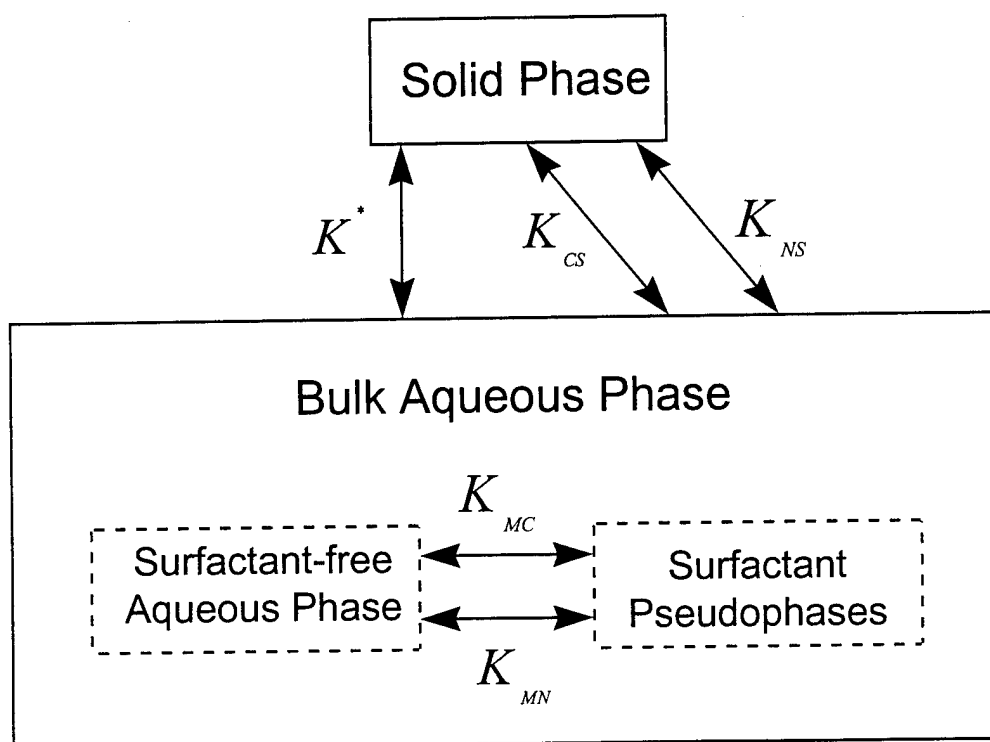
26

Figure 10. Conceptual representation of HOC partitioning in a soil-water system containing micelle-forming cationic and nonionic surfactants.

27

representation when modeling contaminant transport. Equation (14) can be rewritten to accommodate the addition of a cationic surfactant to the system:

$$K^* = K_d \frac{(1 + \kappa_{OC,NS} X_{OC,NS} + \kappa_{OC,cs} X_{OC,cs})}{(1 + K_{MN} C_{MN,a} + K_{MC} C_{MC,a})} \qquad (15)$$

where $X_{OC,cs}$ [$M_{cs}M_{OC}^{-1}$] represents the sorbed cationic surfactant mass per unit mass of soil organic carbon, and $\kappa_{OC,cs}$ [$M_{OC}M_{cs}^{-1}$] is the partitioning coefficient for the HOC between the sorbed cationic surfactant and the soil organic carbon. Both the cationic and nonionic surfactants are micelle-forming; however, the effects on HOC partitioning due exclusively to either cannot be differentiated. Thus, the denominator in Equation (15) can be written as in Equation (14), with the understanding that values for the parameters K_{MN} and K_{MC} will depend on the type of surfactant mixture (i.e., nonionic and cationic surfactant mixture, or nonionic surfactant alone).

For illustrative purposes, partitioning of the nonionic and cationic surfactants are shown in Figure 10 as equilibrium processes; however, there is evidence that they are rate-limited, with slow desorption being the mass-transfer limiting step controlling the distribution of the cationic surfactant (5, 40). Thus for naturally low OC content soils modified with a cationic surfactant, the initial OC content will be due to the modification process (and can be considered essentially constant). Further, because slow desorption controls the aqueous cationic surfactant concentration (following sufficient flushing to remove the high concentration pulse required to establish the enhanced sorbent zone), a relatively constant, low aqueous cationic surfactant concentration will persist within this zone. With these considerations, Equation (15) can be rewritten as:

$$K^* = K_d \frac{(1 + \kappa_{pm,NS} C_{NS,s})}{(1 + K_{MN} C_{MN,a} + K_{MC} C_{MC,a})} \qquad (16)$$

where $\kappa_{pm,NS}$ [$M_{pm}M_{NS}^{-1}$] is the partitioning coefficient for the HOC between the sorbed nonionic surfactant and the bulk solid phase (includes sorbed cationic surfactant), and $C_{NS,s}$ [$M_{NS}M_{pm}^{-1}$] is the sorbed nonionic surfactant concentration. Representing the numerator in Equation (16) in terms of the bulk aquifer material allows this equation to be more easily coupled to a dynamic transport model (40). Note that by assuming a constant OC content resulting from cationic surfactant modification of the soil, K_d becomes redefined as the cationic surfactant modified soil-water distribution coefficient for the HOC. If it is further assumed that partitioning of the nonionic surfactant between the aqueous and solid phase is an equilibrium process (as shown in Figure 10), then $C_{NS,s}$ can be replaced by the appropriate linear or nonlinear partitioning function, and K^* becomes a function of the aqueous nonionic surfactant concentration, $C_{NS,a}$ [$M_{NS}L_a^{-3}$], alone. Below the CMC, aqueous surfactant molecules exist primarily as monomers. Thus, Equation (16) can be rewritten in terms of $C_{NS,a}$ and the aqueous surfactant CMC:

$$K^* = K_d \frac{(1 + \kappa_{pm,NS}C_{NS,s})}{(1 + K_{MN}C_{NS,a})} \ , \ C_{NS,a} \leq CMC \tag{17a}$$

$$K^* = K_d \frac{(1 + \kappa_{pm,NS}C_{NS,s})}{[1 + K_{MN}CMC + K_{MC}(C_{NS,a} - CMC)]} \ , \ C_{NS,a} > CMC \tag{17b}$$

If HOC partitioning into the monomer pseudophase is negligible (i.e., presence of monomers does not affect HOC aqueous solubility) then K_{MN} is equal to zero and Equation (17) reduces accordingly.

2. Chemicals

Milli-Q reagent-grade water (Millipore Corporation, Bedford, MA) containing 0.02% sodium azide (NaN_3) was used in all experiments. NaN_3 was added to inhibit microbial growth and to provide ionic strength to minimize dispersal of fine soil particles during the column transport experiments.

1,2,4-trichlorobenzene (Aldrich Chemical Company; 99% + purity) was used as a representative HOC. TCB solutions used in all experiments were prepared by dilution from saturated stock solutions. Saturated TCB aqueous solutions were prepared using an equilibrator flask (41). The flask was gently stirred in a constant temperature bath (20° C) until saturation was achieved (approximately 48 hours). The aqueous phase was then removed and diluted accordingly prior to use.

Hexadecyltrimethylammonium Chloride (HDTMA; Aldrich; 25 weight % solution in water) was used to modify the representative aquifer material.

IGEPAL CO-730 (Rhone-Poulenc) was use for remobilizing sorbed TCB. A nonionic surfactant was chosen in order to reduce interactions of the mobilizing surfactant with other components of the system. CO-730 is a molecularly nonhomogeneous mixture of polyoxyethylated nonylphenols with an average chemical formula of C_9H_{19}-C_6H_4-O-$(CH_2CH_2O)_{14}CH_2CH_2OH$.

3. Surface Tension Measurements

Surface tension was measured in soil-water-(CO-730) systems using both HDTMA-treated and untreated soils to determine CMC's. Also, surface tension in a water-(CO-730) system with and without a low aqueous concentration of HDTMA was measured. Samples were prepared in duplicate. Soil-water-(CO-730) samples were prepared by placing 5 g of soil and dilutions of a CO-730 stock solution (100 g/L) into 25 mL serum

vials which were then sealed with Teflon®-lined septa. CO-730 concentrations ranged from 0 to 100 g/L. The mixtures were equilibrated on a roller drum at approximately 8 rpm for 48 hours at room temperature (23° C) and then centrifuged at 1500 rpm for 30 minutes. Approximately 10 mL of supernatant was then carefully removed using disposable pipets for surface tension measurement. For the water-(CO-730) samples, surface tension was measured for dilutions of stock CO-730 solution ranging from 0 to 100 g/L. Water-(CO-730) samples with a background HDTMA concentration were prepared by diluting a stock 100 g/L CO-730 with Milli-Q water containing 7 ppm HDTMA. Dilutions ranged from 0 to 100 g/L CO-730. In all cases, surface tension was measured using the drop-weight method (42). Aqueous CO-730 concentrations were measured using a Cary UV-Visible Model 3E spectrophotometer at 274 nm.

4. Sorption Isotherms

Batch sorption isotherm experiments were performed to determine the equilibrium partitioning behavior of CO-730 using both HDTMA-treated and untreated soil. For both cases, batch vials were prepared in triplicate by placing 5 g of soil and dilutions of a CO-730 stock solution (100 g/L) into 25 mL serum vials and sealing with Teflon®-lined septa. CO-730 concentrations ranged from 0 to 100 g/L. The mixtures were equilibrated on a roller drum at approximately 8 rpm for 48 hours at room temperature (23° C) and then centrifuged at 1500 rpm for 30 minutes. Supernatant from each vial was carefully removed, and equilibrium aqueous CO-730 concentrations were measured using the spectrophotometric method previously described. Equilibrium sorbed phase concentrations were calculated by difference.

Batch sorption isotherm experiments were performed to determine the equilibrium partitioning behavior of TCB as a function of aqueous CO-730 concentration. Only soil treated with HDTMA was used in these experiments. Batch vials were prepared by placing 5 g of soil into 25 mL serum vials, filling to capacity with solutions containing TCB and CO-730, and sealing with Teflon®-lined septa. For a given initial CO-730 concentration (ranging from 0 to 40 g/L), initial TCB concentrations ranged from 0.015 to 22.7 ppm. Four samples (two with soil and two without) were prepared for each initial TCB concentration. The mixtures were equilibrated on a roller drum at approximately 8 rpm for 48 hours at room temperature (23° C) and then centrifuged at 1500 rpm for 30 minutes. 20 μL Aliquots of supernatant were removed from each vial and spiked into autosampler vials containing 1 mL of acetonitrile and an internal standard (10 ppm 1,4-dichlorobenzene; Aldrich). Two analysis vials were prepared for each sample vial. These analysis vials were sealed with Teflon®-lined septa and analyzed for TCB using a Hewlett-Packard 5890 II gas chromatograph with a DB-1 capillary column (15 m x 0.53 mm, 3 μm film thickness) and a [63]Ni electron capture detector. Helium was used as a carrier gas, with a flow rate of 3.72 mL/minute. The detector temperature was set at 280° C, and the injection temperature was 120° C. The oven program was as follows: 50° C for 2 min, ramp to 200° C at 30° C/min, 0.25 min final hold. Sorbed-phase concentrations were calculated by difference.

5. HOC Solubility in Presence of Aqueous Surfactant

Experiments were conducted to quantify the change in TCB aqueous solubility as a function of aqueous CO-730 concentration, for solutions with and without a background HDTMA concentration. Excess TCB was placed into equilibrator flasks (41) containing aqueous solutions of known CO-730 concentrations. The flasks were then gently stirred in a constant temperature bath (20° C) for 48 hours. Aqueous samples were prepared and analyzed for TCB as described above.

6. Nonionic Surfactant Transport in Soil Columns

The transport behavior of CO-730 in a flow-through system was studied using one-dimensional column experiments. The purpose of these experiments was to determine whether differences in CO 730 transport would occur between HDTMA-treated and untreated aquifer material systems under dynamic flow conditions. Two experiments were performed: one using soil treated with HDTMA, and one using untreated soil. For each experiment, porous media was dry-packed into a stainless steel column (25 cm in length; 2.1 cm in diameter) and capped with 2 μm stainless steel end frits. The column was then purged with CO_2 to minimize trapped air, and saturated with water. An ISCO model 2350 HPLC pump was used to deliver fluids to the column. *In situ* soil porosity was estimated using $\theta=(M_W-M_D)/\rho_W V_c$, where θ=soil porosity, M_W=mass of water saturated soil-filled column (g), M_D=mass of dry soil-filled column (g), ρ_W=density of water (~1 g/mL at 20° C), and V_c=bulk volume of the column (mL). The columns had measured porosities of $\theta=0.35$ for the untreated soils, and $\theta=0.4$ for the treated soil. The difference in measured porosities is likely due to the natural variation in the grain size of the aquifer material. To begin an experiment, a pulse of 50 g/L CO-730 solution was introduced into the upgradient end of the column for 5 hours, at a constant flow rate (Q) of 0.25 mL/min. This pulse was followed by 20 hours of flushing with surfactant-free water, also at a constant flow rate of 0.25 mL/min. This flow rate corresponds to a constant average pore water velocity (v) of 12.4 cm/hr for the untreated soil and 10.91 cm/hr for the treated soil, using $v=Q/\theta A$, where A is the column cross section area (3.5 cm^2); these pore water velocities are within the range of those observed at the Columbus, MS site (22). Throughout an experiment, liquid samples were collected at the column outlet (6 minute collection time per sample), using a Gilson Model 212B fraction collector. Liquid samples were then analyzed for aqueous CO-730 concentration, using the spectrophotometric method previously described.

31

7. HOC Immobilization and Recovery in Soil Columns

A one-dimensional column experiment was performed to demonstrate the feasibility of remobilizing TCB immobilized within a cationic surfactant-enhanced (HDTMA) sorbent zone using nonionic surfactant (CO-730) flushing. For this experiment, HDTMA-treated porous media was dry packed into a stainless steel column as in the CO-730 transport experiments. The soil had a measured porosity of θ=0.46. After establishing a steady flow of water at 0.25 mL/min (v=9.42 cm/hr), a 5-hour pulse of 16.44 ppm TCB was introduced into the upgradient end of the column. An ISCO LC 5000 syringe pump was used to deliver the TCB pulse in order to minimize volatilization losses. This pulse was followed by 65 hours of flushing with TCB-free water, also at a constant flow rate of 0.25 mL/min. During the period of water flushing, liquid samples were collected periodically from the column outlet and analyzed for TCB. The collection time for a sample was 6 minutes. Immediately after a sample was collected, duplicate analysis samples were prepared by adding 20 µL aliquots of the collected sample to autosampler vials containing 1 mL of acetonitrile and an internal standard (10 ppm 1,4 dichlorobenzene). These samples were then analyzed using GC as previously described. Controls indicated that volatile losses of TCB during the 6 minutes required to collect a sample from the column were negligible. Following the water flushing, a continuous flow of 50 g/L CO-730 (at 0.25 mL/min) was initiated and continued for 30 hours. During the first 9 hours of surfactant flushing, samples were collected on 6- or 12-minute intervals (12 minute intervals during early TCB breakthrough at the column outlet, 6-minute intervals during the maximum breakthrough and roll-off period). During the remaining 21 hours, samples were collected on time intervals ranging from approximately 20 minutes to 2.8 hours. Samples collected during the surfactant flushing period were analyzed for TCB as previously described. These samples were also analyzed for CO-730 concentrations using the spectrophotometric method previously described.

B. RESULTS

Equilibrium sorption isotherms for CO-730 using HDTMA treated and untreated soils are shown in Figure 11. Sorption of CO-730 is highly nonlinear for both, with the nonlinearity being more pronounced for the treated soil. The strong sorption at low aqueous concentrations, as well as the higher maximum sorption capacity of the treated soil follows from the properties of surfactants. Surfactants are surface-active substances and have an affinity for interfaces, such as solid-aqueous phase interfaces. At the solid-water interface, the surfactant molecules tend to orient themselves with the hydrophilic portion in the aqueous phase and the hydrophobic portion at the interface or possibly within a hydrophobic surface layer, yielding non-linear sorption behavior. The untreated Columbus aquifer material has very little OC content. Increasing its OC content by a factor of 5 using HDTMA (a more effective hydrophobic sorbent than natural OC) resulted in a modest but significant increase in sorption of CO-730. This
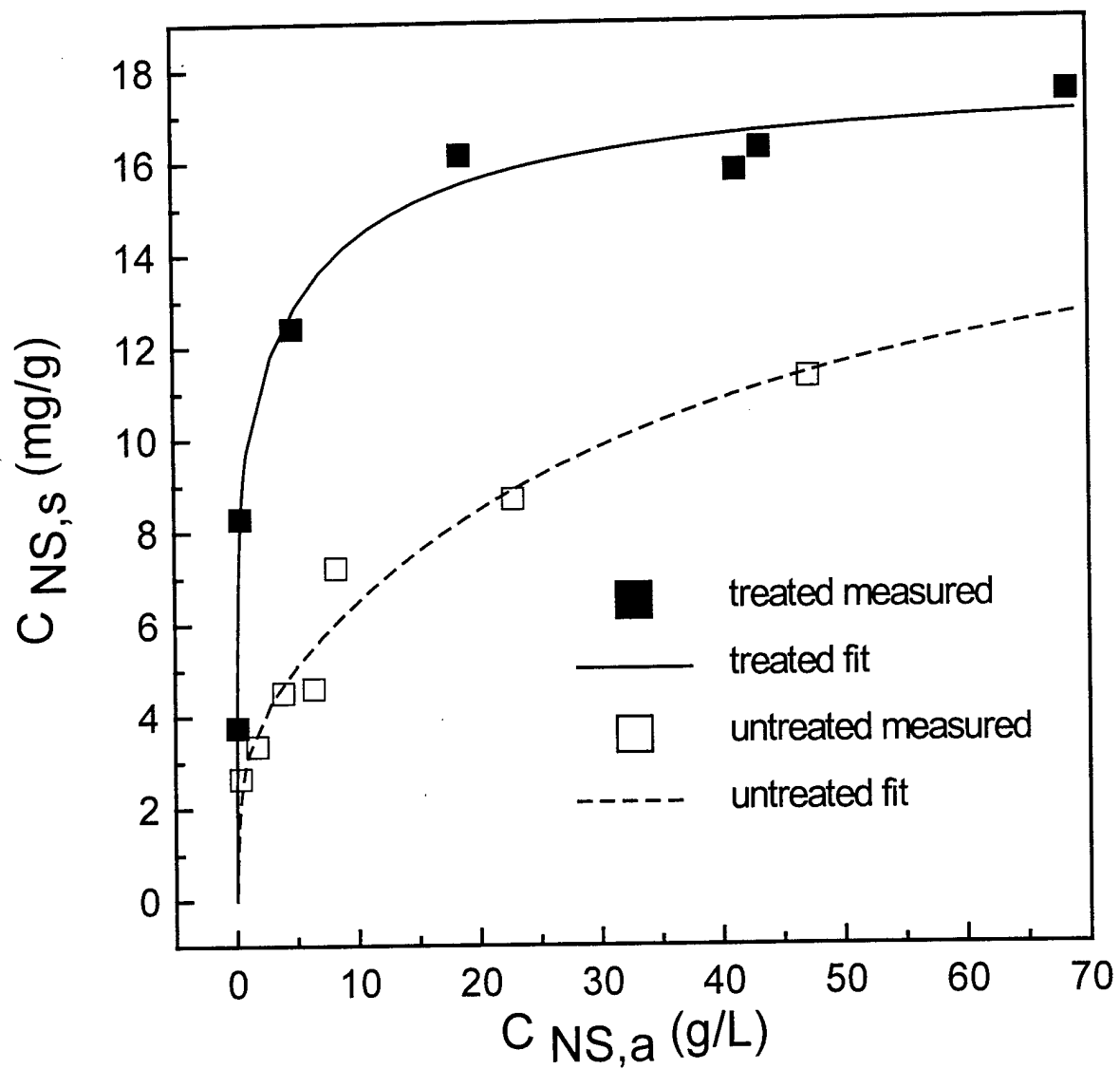
32

Figure 11. Equilibrium sorption isotherms for CO-730 on HDTMA-treated and untreated Columbus soil.

suggests that CO 730 transport will be retarded in HDTMA-modified aquifer material verses unmodified aquifer material, but this effect will likely be minor. Figure 11 also shows fitted curves to the sorption data, obtained using the two-term Langmuir equation:

$$C_{NS,s} = \frac{b_1 k_1 C_{NS,a}}{1 + k_1 C_{NS,a}} + \frac{b_2 k_2 C_{NS,a}}{1 + k_2 C_{NS,a}} \tag{18}$$

where b_1, k_1, b_2, and k_2 are fitting parameters, summarized in Table 2. It should be emphasized that the use of Equation (18) to model these partitioning data is not based on mechanistic grounds, but on the established fact that any sorption reaction represented by data such as those in Figure 11 can be mathematically represented in this way (43). Thus, as is the case for many partitioning relationships, Equation (18) should be viewed as an interpolation equation with four fitting parameters calibrated using experimental data. In fitting these curves we used a graphical technique (43) to obtain initial values, and then optimized these values using LM nonlinear parameter estimation (26).

Table 2. Two-Term Langmuir Coefficients for CO-730 Equilibrium Sorption Isotherms Using HDTMA-Treated and Untreated Columbus Aquifer Material

Soil Type	b_1 (mg/g)	b_2 (mg/g)	k_1 (mL/mg)	k_2 (mL/mg)
Untreated	3.61	13.85	3.42	0.03
Treated	9.71	8.03	9.51	0.15

Measurements of aqueous phase surface tension as a function of aqueous CO-730 concentration for soil-water-(CO-730) systems (HDTMA-treated and untreated soils) and for water-(CO-730) systems (with and without a small aqueous concentration of HDTMA) are shown in Figure 12. Approximate CMC values for each system can be estimated as the value of $C_{NS,a}$ at which the pronounced break between the two relatively linear regions of each data set occurs (29). It is clear from Figure 12 that defining the CMC in this way is subjective, especially for the systems containing soil or aqueous HDTMA. This general trend has been noted by previous researchers using molecularly nonhomogeous surfactants (39, 12) and is thought to partially result from sequential micellization of the heterogeneous monomers due to their variable water solubilities. The presence of the soil phase likely contributes to this sequential micellization by selectively sorbing the more hydrophobic surfactant monomers. For example, the CMC for the aqueous CO 730/water system is ~10 g/L, while the CMC for the untreated soil/CO 730/water system is ~0.8 g/L. To simulate the effect of the aqueous phase HDTMA concentration (3-7 ppm) expected to be present in a fully
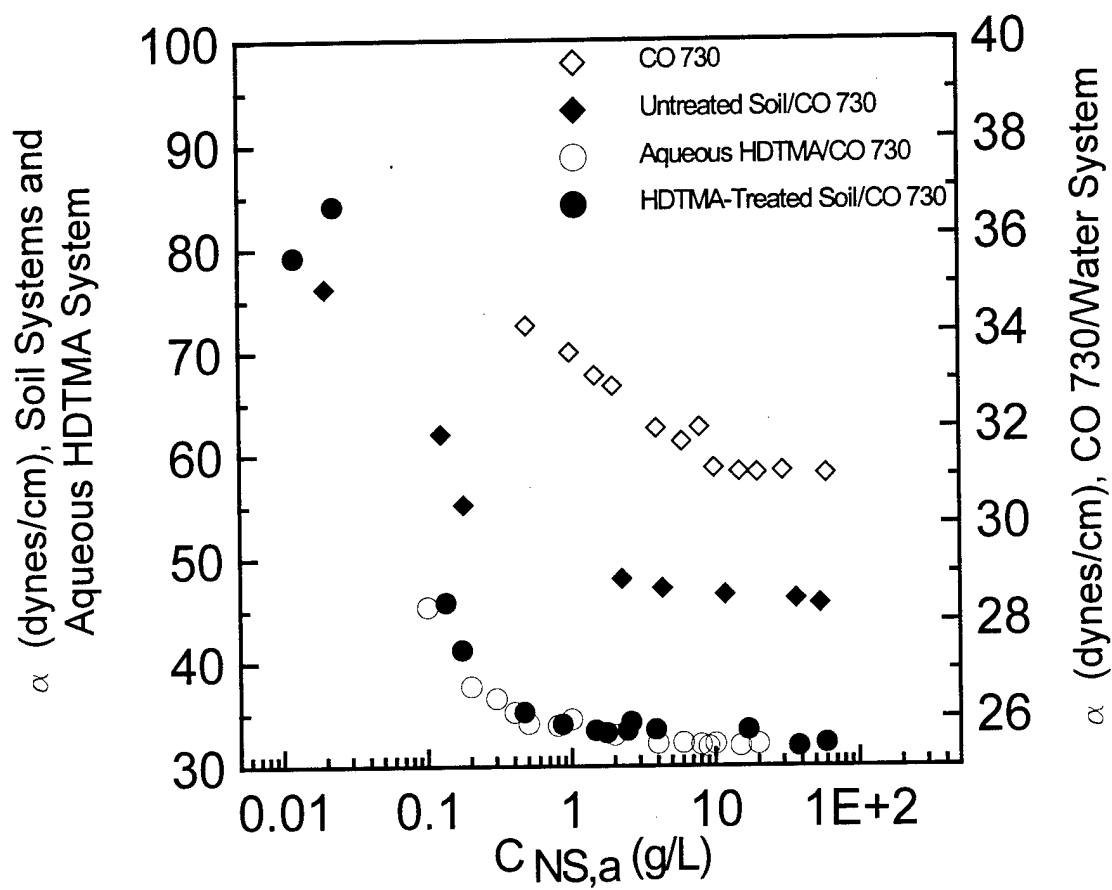
34

Figure 12. Surface tension (α) as a function of aqueous CO-730 concentration for soil water-(CO-730) and water-(CO-730) systems (with and without 7 ppm HDTMA).

developed enhanced sorbent zone (5), 7 ppm HDTMA was added to the soil-free system. This concentration is much smaller than the CMC for HDTMA alone in aqueous solution (~300 ppm) (7); therefore, it can be assumed that all of the HDTMA was initially present as cationic surfactant monomers. Data from the system containing aqueous HDTMA and the system containing HDTMA-treated soil are remarkably similar (0.3 g/L < CMC < 0.7 g/L), suggesting that the presence of a small aqueous HDTMA concentration has a significant influence on micelle formation. This reduction in the apparent CMC in the presence of low aqueous HDTMA can be attributed to non-ideal mixed micelle formation (45, 46), a phenomenon which occurs when surfactants with dissimilar head groups are mixed. In this case, the nonionic surfactant head groups repel one another on average more than they are repelled by the cationic surfactant head groups; similarly, the cationic surfactant head groups repel one another on average more than they are repelled by the nonionic surfactant head groups. This interaction results in the formation of mixed (i.e., cationic and nonionic surfactant) micelles at a CMC lower than the CMC's for either of the surfactants alone.

The change in apparent aqueous TCB solubility as a function of the aqueous CO-730 concentration is shown in Figure 13, for systems with and without 7 ppm HDTMA. In both cases the data are bilinear; the marked increase in slope indicating the presence of a micellar pseudophase. As in Figure 13, the value of $C_{NS,a}$ corresponding to the break in the curves approximates the CMC; however, in Figure 13 these breaks are much better defined (~0.6 g/L and ~10 g/L for systems with and without HDTMA, respectively). Figure 13 suggests that in these systems solubility enhancement is a much more sensitive indicator of the monomer-micelle transition than changes in surface tension; an observation which has been previously noted by researchers studying similar systems (12). Thus, in subsequent calculations a CMC of 0.6 g/L for systems containing HDTMA-treated soil is used. Previous studies (12, 13) have shown that the sub-CMC slope (s_1) is related to the HOC partitioning coefficient between the surfactant monomer pseudophase and the bulk aqueous phase, while the supra-CMC slope (s_2) is related to the HOC partitioning coefficient between the surfactant micellar pseudophase and the bulk aqueous phase. As defined in Equation (16), these relationships can be written as $K_{MN}=s_1/S_w$ and $K_{MC}=s_2/S_w$, where S_w is equal to the aqueous solubility of the HOC in surfactant-free water. For the system containing HDTMA shown in Figure 13, K_{MN} and K_{MC} are estimated as 1.04 L/g and 4.4 L/g, respectively, using a measured value of S_w=16.74 ppm.

An interesting observation arising from Figure 13 is the dramatic difference in the two systems in TCB solubility upon the onset of micellization. Although it is difficult to state conclusively, we speculate that this effect is related to the number and nature of the micelles formed in the two systems. In the system containing aqueous HDTMA, micellization occurs at a lower total surfactant concentration; hence less micelles are available for TCB solubilization compared to the system containing only aqueous CO 730. Also, previous researchers (12) have speculated that for ionic surfactants,
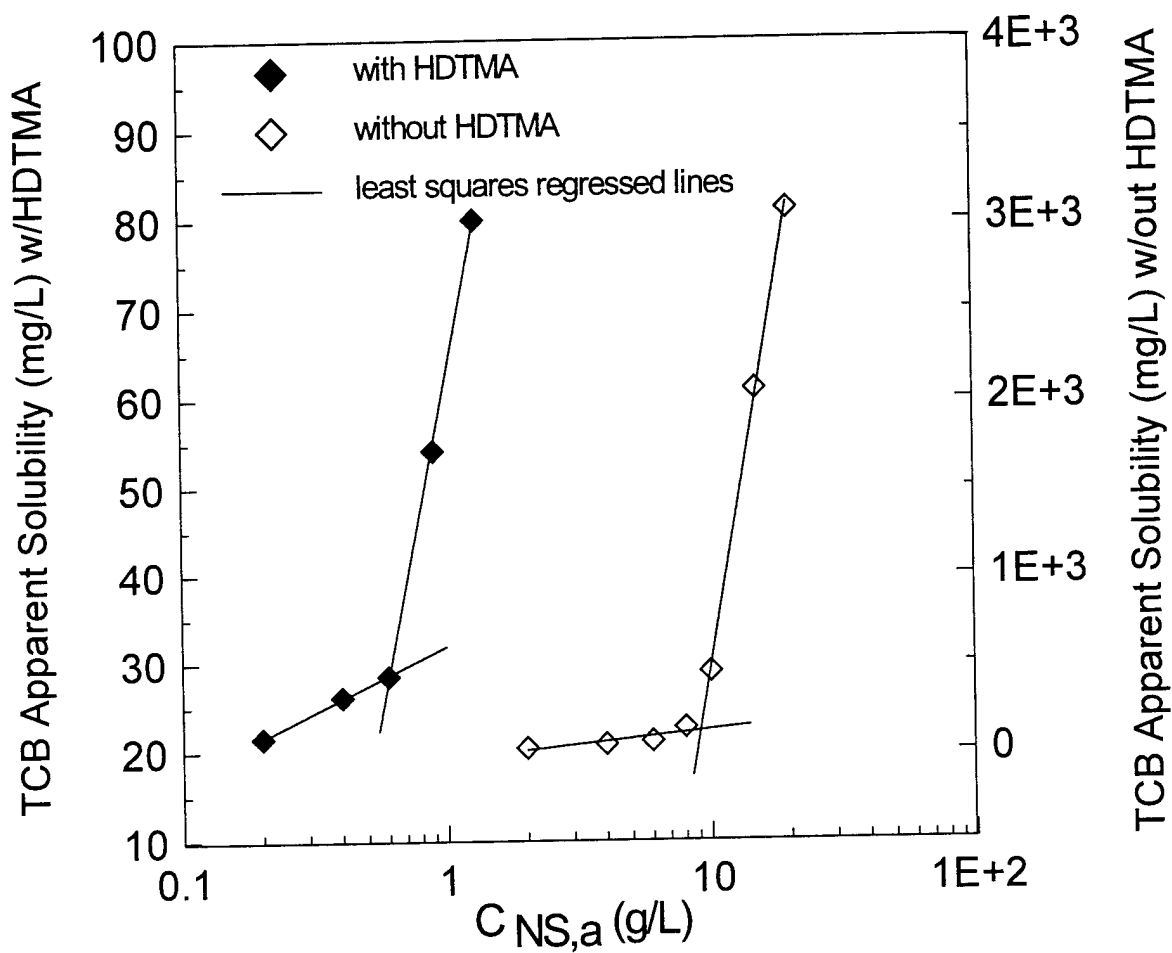
Figure 13. Apparent aqueous solubility of TCB as a function of aqueous CO-730 concentration in water-(CO-730) systems with and without 7 ppm HDTMA.

37

differences in organic solute solubility may be a result of reduced accessibility of the interior of the micelle to the solute resulting from hydration of the outer, polar zone of the micelle. If this effect occurs in systems containing ionic micelles, then it is reasonable to expect that hydration of mixed ionic and nonionic micelles will also result in reduced organic solute solubility.

Equilibrium sorption isotherms for TCB on HDTMA-treated soil at different aqueous CO-730 concentrations are shown in Figure 14. These isotherms were linear over the concentration range studied, with the slope of each being equal to the apparent partitioning coefficient (K^*) at their respective aqueous CO-730 concentrations. In Figure 15, values for K^* from Figure 14 are shown as a function of the aqueous CO-730 concentration. Values at aqueous CO-730 concentrations below the apparent CMC (~ 0.6 g/L) are greater than when no CO-730 is present. A dramatic drop in K^* occurs at CO-730 concentrations greater than the CMC. Similar trends have been noted by other researchers considering HOC sorption in the presence of nonionic surfactants (39). This behavior likely results from an increase in the solid phase OC content due to nonionic surfactant sorption at sub-CMC aqueous concentrations. As the aqueous nonionic surfactant concentration exceeds the CMC, the formation of a micellar pseudophase provides a more favorable partitioning medium for the HOC, and K^* decreases. The results shown in Figure 15 are encouraging from the perspective of an enhanced sorption/enhanced remobilization remediation scheme, because they suggest that HOC partitioning to the mobile micellar phase is favorable even in soils having a large OC content due to treatment with cationic surfactants.

Also shown in Figure 15 is a curve fit to the K^* versus $C_{NS,a}$ data, obtained using Equations (17a), (17b), and (18). Before applying these equations, a value for $\kappa_{pm,NS}$ (the HOC partitioning coefficient between the sorbed nonionic surfactant and the remainder of the solid phase) was required; however, it is not possible to measure this value independently. In our case we used the measured data in Figure 15, values for the parameters measured in our batch experiments (b_1, k_1, b_2, and k_2 from Figure 11 and Equation (18) (Table 2); K_{MN} and K_{MC} from Figure 14) and LM nonlinear parameter estimation to estimate a value for $\kappa_{pm,NS}$ of 0.59 g/mg. The 90% confidence intervals are also plotted in Figure 15, based on a least squares-determined standard error for $\kappa_{pm,NS}$ of 0.07 g/mg. A value for $\kappa_{pm,NS}$ less than 1 suggests that the HDTMA-treated soil is a more favorable partitioning medium for TCB than any CO 730 sorbed to the solid phase.

Effluent breakthrough curves for CO-730 in HDTMA-treated and untreated soil columns are shown in Figure 16. These curves are plotted as a function of total column pore volumes, where 1 pore volume=vt/x, and x is the porous medium transport length (25 cm). By nondimensionalizing the abscissa, a direct comparison can be made between these curves. CO-730 breakthrough is slightly retarded in the treated soil compared to the untreated soil. This is expected because of the increase in OC in the HDTMA-
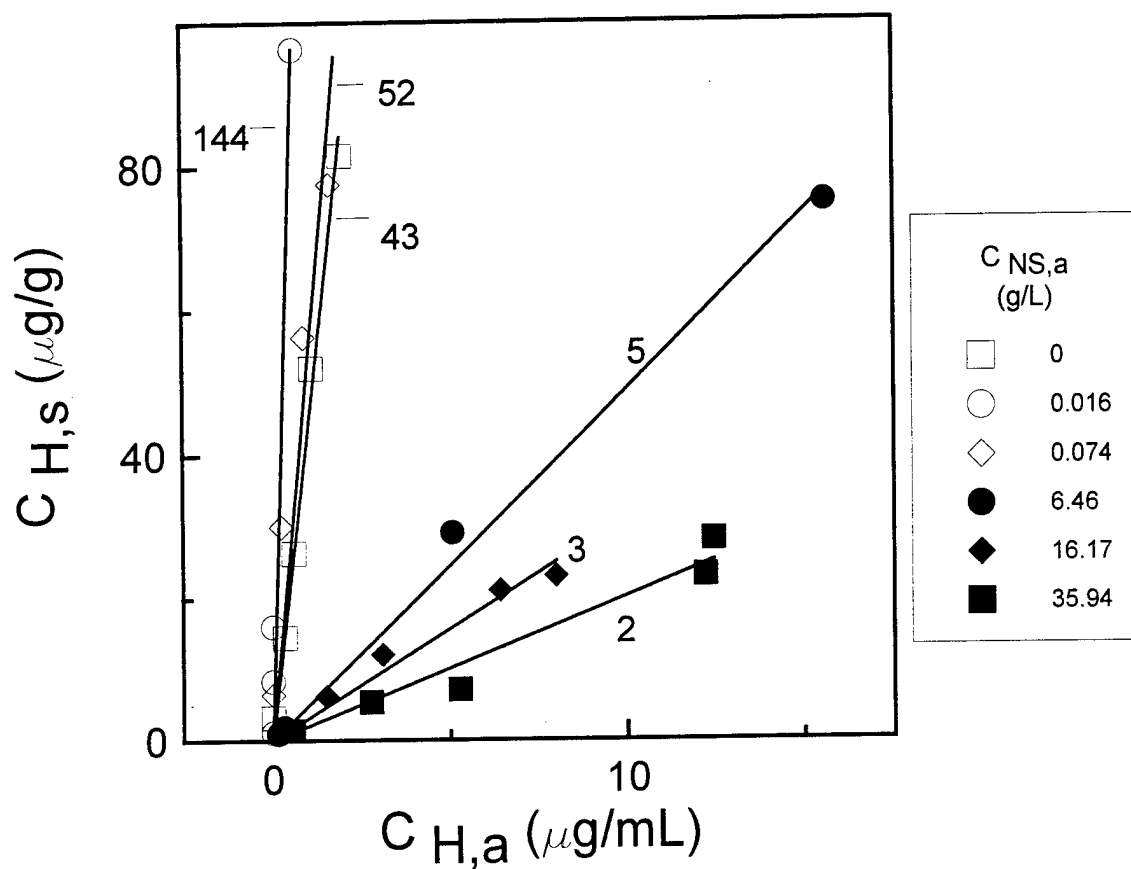
Figure 14. Equilibrium sorption isotherms for TCB on HDTMA-treated Columbus soil as a function of aqueous CO-730 concentration. Apparent sorption coefficients are indicated.
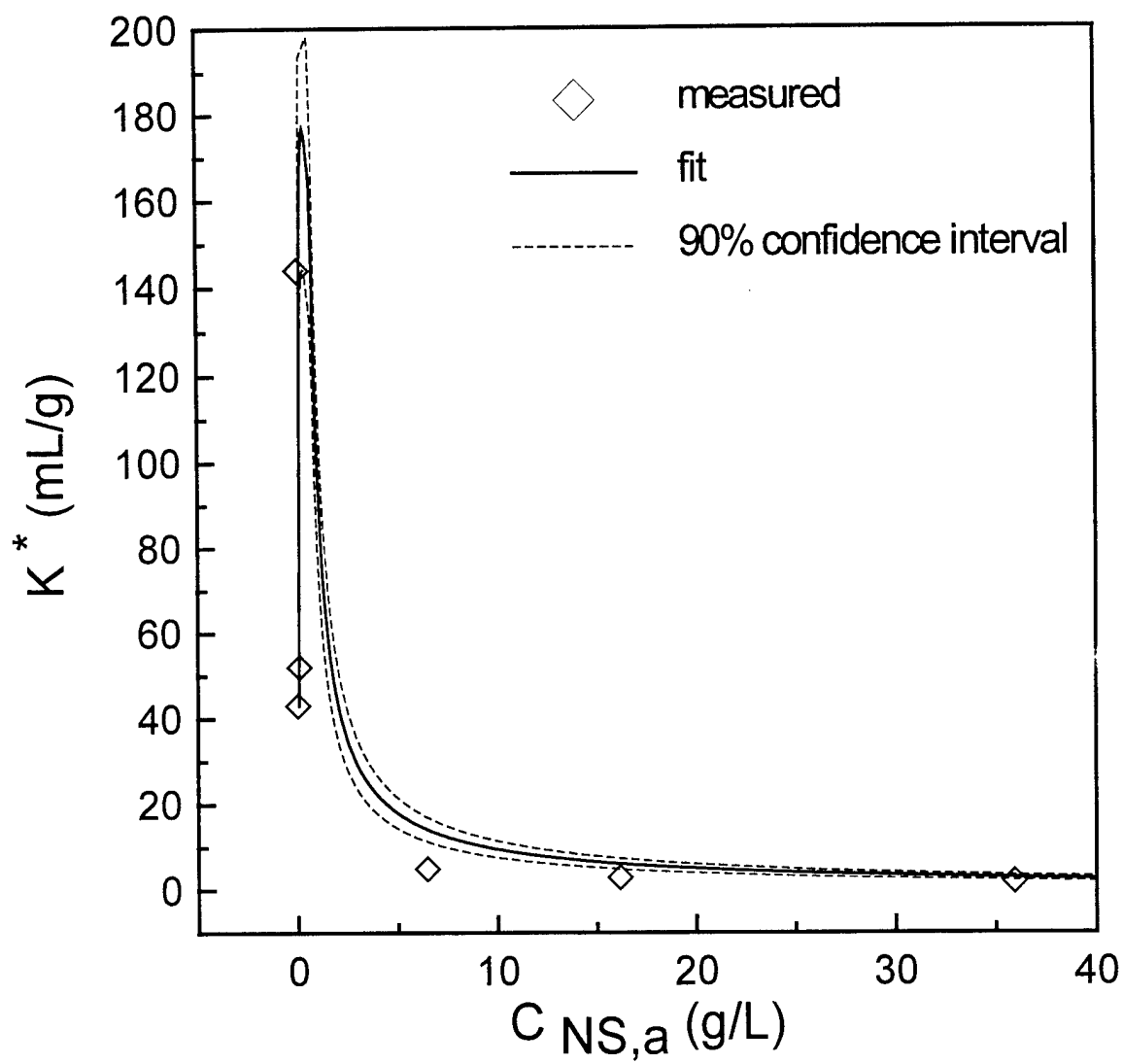
Figure 15. Apparent equilibrium distribution coefficients (K*) for TCB on HDTMA-treated soil as a function of aqueous CO-730 concentration.
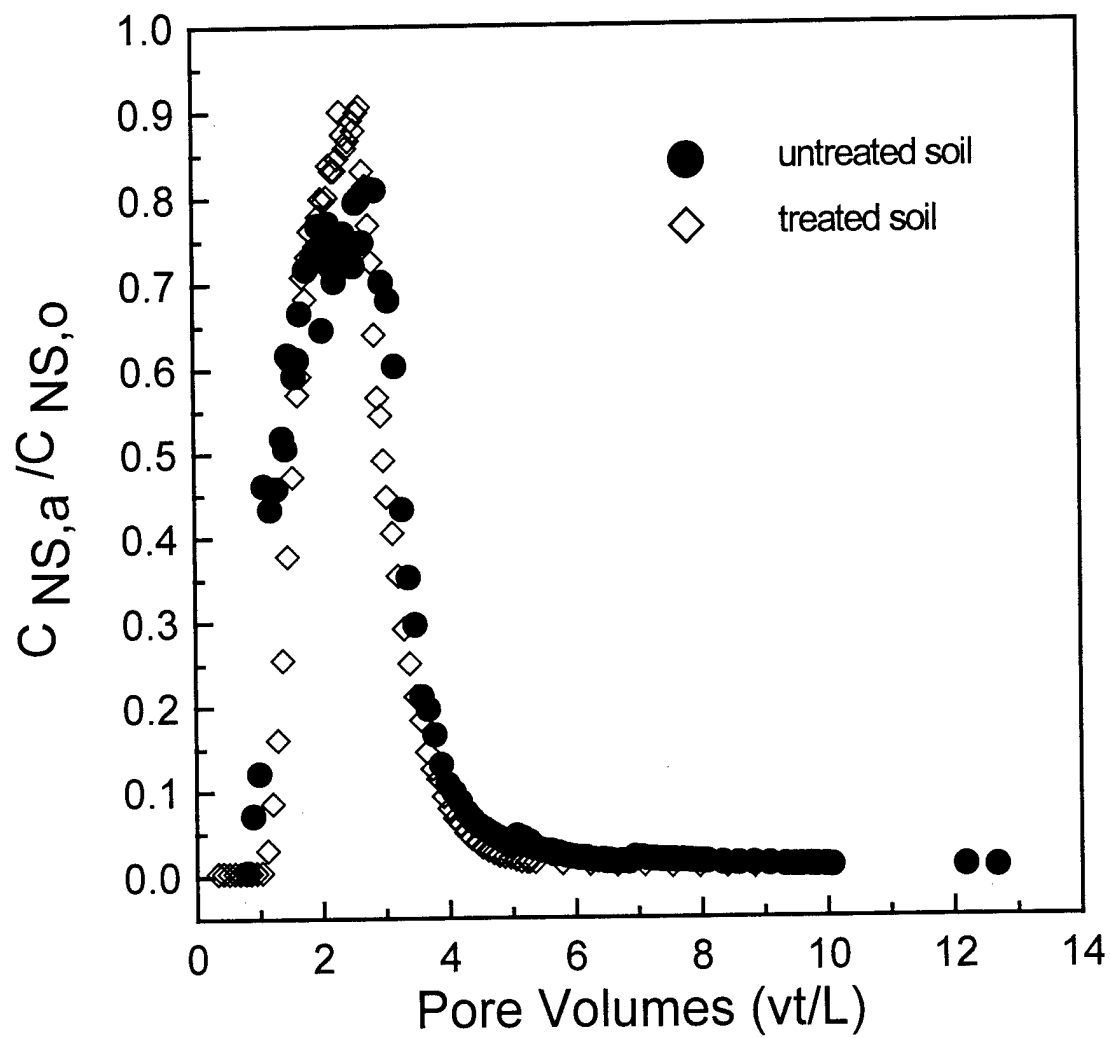
Figure 16. Effluent breakthrough curves for CO-730 in HDTMA-treated and untreated Columbus soil columns.

treated soil relative to the untreated soil. Nevertheless, the slight difference in these curves suggests that the presence of sorbed and aqueous HDTMA has a minor effect on the transport behavior of CO-730.

Effluent breakthrough curves for TCB and CO-730 in an HDTMA-treated soil column are shown in Figure 17. These curves are also shown as a function of column pore volumes. In this experiment, a 5-hour pulse (~1.9 column pore volumes) of TCB was followed by a period of flushing with clean water (~25 pore volumes), during which no TCB was detected in the column effluent. Following this flushing, a continuous input of CO-730 (50 g/L) was initiated. Breakthrough of both the TCB and the CO-730 occurred simultaneously, indicating a rapid remobilization of the sorbed TCB. The failure of the normalized CO 730 concentrations to reach a plateau value of one is likely a measure of the error in the CO 730 analysis method (~5%). Greater then 99% of the TCB mass was recovered after flushing with approximately 12 pore volumes of CO-730 solution. In contrast, to achieve this level of TCB recovery by flushing with clean water alone would require in excess of 400 pore volumes *(40)*. Figure 17 illustrates the feasibility of remobilizing an HOC (TCB) from within an HDTMA-modified enhanced sorbent zone using surfactant-enhanced solubilization with a nonionic surfactant (CO-730) in a one-dimensional flow regime.
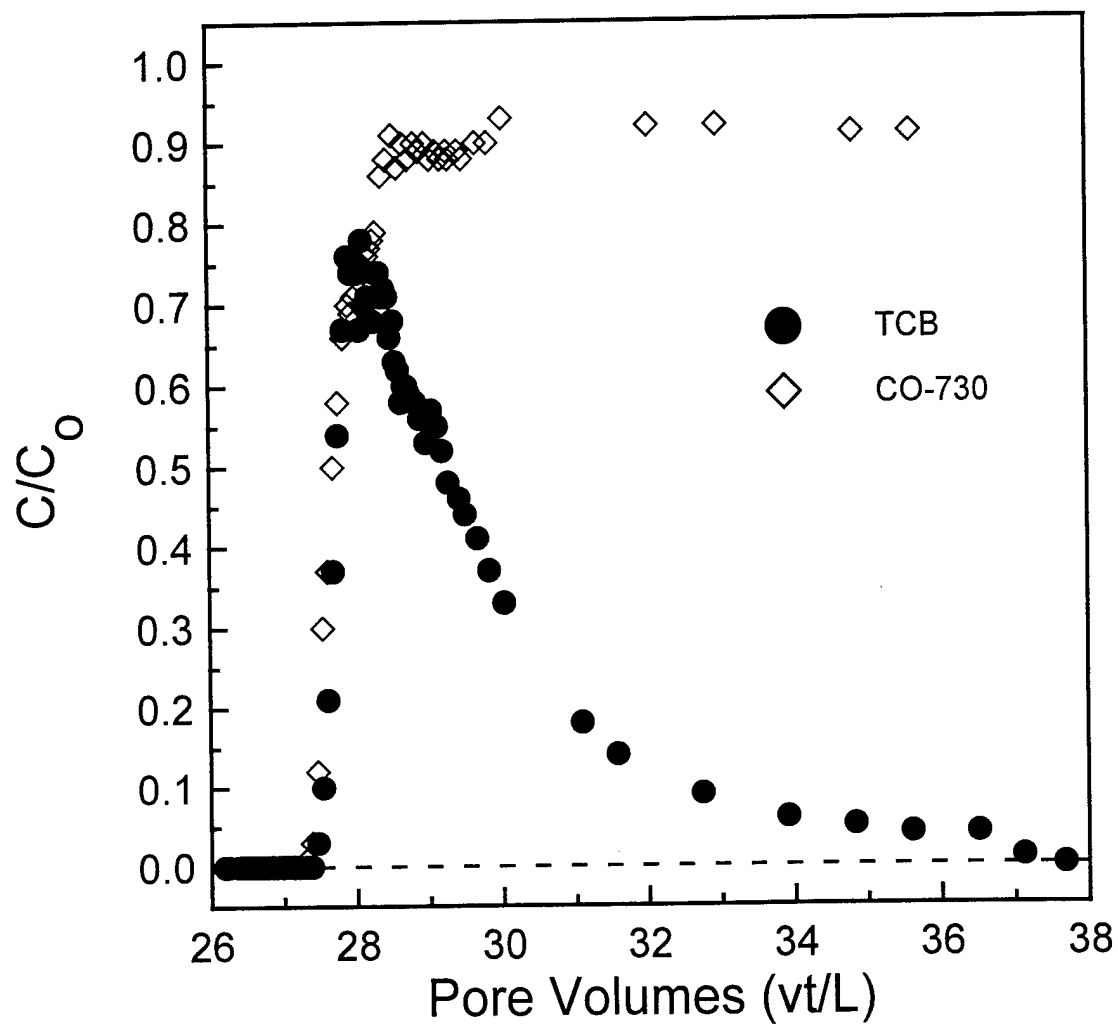
Figure 17. Effluent breakthrough curves for CO-730 and TCB in an HDTMA-treated Columbus soil column.

SECTION V

NONIONIC SURFACTANT-ENHANCED SOLUBILIZATION OF HOCs FROM WITHIN CATIONIC SURFACTANT-ENHANCED SORBENT ZONES: SIMULATIONS

A. METHODOLOGY

1. Model Development

With reference to Figure 10, TCB partitioning between the bulk aqueous phase and the solid phase can be described by (47):

$$C_{H,s} = K^* C_{H,a} \tag{19}$$

$$K^* = K_d \frac{(1 + \kappa_{pm,NS} C_{NS,s})}{(1 + K_{MN} C_{NS,a})} \, , \quad C_{NS,a} \leq CMC \tag{20a}$$

$$K^* = K_d \frac{(1 + \kappa_{pm,NS} C_{NS,s})}{[1 + K_{MN} CMC + K_{MC}(C_{NS,a} - CMC)]} \, , \quad C_{NS,a} > CMC \tag{20b}$$

In the above equations, K^* is a function of $C_{NS,a}$ and $C_{NS,s}$. Batch and column experiments described in (47) allowed for direct measurement of the parameters in Equation (20) save $\kappa_{pm,NS}$, which was determined indirectly using LM nonlinear parameter estimation (26; see Table 3). The presence of a small aqueous concentration of HDTMA, resulting from treatment of the aquifer material to simulate a cationic surfactant-enhanced sorbent zone, causes non-ideal mixed micelle formation with CO-730 (47). Systems incorporating a small aqueous HDTMA concentration were used to determine K_{MN}, K_{MC}, and CMC.

To use Equations (19) and (20) to model TCB partitioning in the presence of the nonionic surfactant CO-730, a relationship describing CO-730 partitioning between the bulk aqueous phase and the solid phase is required. Batch sorption experiments performed in (47) showed that this partitioning could be approximated by the equilibrium two-term Langmuir equation (43):

44

Table 3. Experimentally Determined Model Parameters

Parameter	HDTMA-Treated Aquifer Material	Value
K_d	Yes	43.0 mL/g
K_{MN}	Yes	1.04 L/g
K_{MC}	Yes	4.4 L/g
CMC	Yes	0.6 g/L

$$C_{NS,s} = \frac{b_1 k_1 C_{NS,a}}{1 + k_1 C_{NS,a}} + \frac{b_2 k_2 C_{NS,a}}{1 + k_2 C_{NS,a}} \qquad (21)$$

where b_1, k_1, b_2, and k_2 are fitting parameters (values for these parameters are given in Table 2). If equilibrium partitioning is valid, then Equation (21) allows Equation (20) to be rewritten in terms of $C_{NS,a}$ alone. However, there is evidence that in a dynamic groundwater system this partitioning is mass-transfer limited (47, 48). Thus, a kinetic form of the Langmuir equation was also employed in our modeling study:

$$\frac{\partial C_{NS,s}}{\partial t} = k_f C_{NS,a} (b - C_{NS,s}) - k_b C_{NS,s} \qquad (22)$$

where k_f [$M_{NS}^{-1} L_a^3 T^{-1}$] and k_b [T^{-1}] are fitting parameters describing the forward and reverse sorption rates, respectively, and b [$M_{NS} M_{pm}^{-1}$] is a constant related to the maximum sorptive capacity of the aquifer material (5, 20, 49).

As Equation (20) suggests, TCB and CO-730 transport is a coupled process which can be represented in one-dimension by:

$$\frac{\partial C_{H,a}}{\partial t} + \frac{\rho_b}{\theta} \frac{\partial C_{H,s}}{\partial t} = - v \frac{\partial C_{H,a}}{\partial x} + D_H \frac{\partial^2 C_{H,a}}{\partial x^2} \qquad (23a)$$

$$\frac{\partial C_{NS,a}}{\partial t} + \frac{\rho_b}{\theta} \frac{\partial C_{NS,s}}{\partial t} = - v \frac{\partial C_{NS,a}}{\partial x} + D_{NS} \frac{\partial^2 C_{NS,a}}{\partial x^2} \qquad (23b)$$

where x [L_{pm}] and t [T] are spatial and temporal variables, ρ_b [$M_{pm} L_{pm}^{-3}$] and θ [$L_a^3 L_{pm}^{-3}$] are the dry bulk density and saturated porosity of the aquifer material, respectively; v [$L_a T^{-1}$] is the average pore water velocity; and D_H [$L_{pm}^2 T^{-1}$] and D_{NS} [$L_{pm}^2 T^{-1}$] are the

hydrodynamic dispersion coefficients for TCB and CO-730, respectively. If it is assumed that diffusion of TCB and CO-730 during transport is negligible, then both D_H and D_{NS} can be replaced by $\alpha_L v$, where α_L [L_{pm}] is the longitudinal dispersivity of the aquifer material. The coupling between Equation (23a) and Equation (23b) is apparent when Equation (19) is differentiated with respect to time:

$$\frac{\partial C_{H,s}}{\partial t} = K^* \frac{\partial C_{H,a}}{\partial t} + C_{H,a} \frac{\partial K^*}{\partial t} \tag{24}$$

Thus Equation (23a) can be rewritten:

$$R_H \frac{\partial C_{H,a}}{\partial t} + \frac{\rho_b \, C_{H,a}}{\theta} \frac{\partial K^*}{\partial t} = - v \frac{\partial C_{H,a}}{\partial x} + \alpha_L v \frac{\partial^2 C_{H,a}}{\partial x^2} \tag{25}$$

where:

$$R_H = R_H(C_{NS,a}, C_{NS,s}) = 1 + \frac{\rho_b}{\theta} K^* \tag{26}$$

When equilibrium partitioning of CO-730 is assumed, Equation (23b) can be rewritten as:

$$R_{NS} \frac{\partial C_{NS,a}}{\partial t} = - v \frac{\partial C_{NS,a}}{\partial x} + \alpha_L v \frac{\partial^2 C_{NS,a}}{\partial x^2} \tag{27}$$

where R_{NS} is the nonlinear, equilibrium two-term Langmuir retardation coefficient:

$$R_{NS} = R_{NS}(C_{NS,a}) = 1 + \frac{\rho_b}{\theta} \left[\frac{k_1 b_1}{(1 + k_1 C_{NS,a})^2} + \frac{k_2 b_2}{(1 + k_2 C_{NS,a})^2} \right] \tag{28}$$

For kinetic partitioning of CO-730, Equation (23b) becomes:

$$\frac{\partial C_{NS,a}}{\partial t} = - v \frac{\partial C_{NS,a}}{\partial x} + \alpha_L v \frac{\partial^2 C_{NS,a}}{\partial x^2} - \frac{\rho_b}{\theta} \left[k_f C_{NS,a} (b - C_{NS,s}) - k_b C_{NS,s} \right] \tag{29}$$

46

2. Numerical Method

Simulations investigating the transport behavior of CO-730 (Equations (27), (28), (29)), TCB (Equations (25) and (26), with K^* equal to K_d), and coupled CO-730-TCB (Equations (20), (25)-(29)) in one dimensional columns of HDTMA-treated and untreated Columbus, MS aquifer material were performed utilizing the experimental data presented in *(47)* and in Section IV. Conditions for these simulations are summarized in Table 4. In all cases, the finite-difference, Crank-Nicholson numerical technique was used. Picard iteration *(23)* was used to handle nonlinearities in the partial differential equations. All simulations utilized continuous mass-flux inflow boundary conditions and continuous aqueous concentration outflow boundary conditions. In all cases, initial concentrations throughout the simulation domain (columns) were equal to zero. Numerical dispersion and oscillations were controlled by discretizing the problem so that the grid Peclet and Courant number criteria were satisfied *(23)*. Numerical accuracy of simulation output was evaluated based on comparison with analytical solutions (for the equilibrium partitioning models) and on mass-balance considerations (for both equilibrium and kinetic partitioning models). Mass-balance calculations for both TCB and CO-730 were made by equating the total mass entering and leaving the column to the total mass stored within the column at a given time. The equilibrium partitioning model simulations compared well with analytical solutions; in all simulations the relative mass balance error was below 3%.

3. Model Parameters

In Table 4, simulations A, B, and E correspond to column transport experiments described in *(47)* and in Section IV; simulations C and D are numerical experiments performed to illustrate the expected behavior of TCB in natural aquifer material and within a cationic surfactant-enhanced sorbent zone (C and D, respectively), without nonionic surfactant-enhanced remobilization.

2. RESULTS

Effluent breakthrough curves for simulations A (untreated porous media) and B (HDTMA-treated porous media), utilizing equilibrium two-term Langmuir (Equation (21)) and kinetic Langmuir (Equation (22)) partitioning relationships, are shown in Figures 18a and 18b, respectively. Measured effluent data from *(47)* are also shown in these figures. In these simulations, a pulse of 50 mg/mL CO-730 solution was input into the column for 5 hours at a volumetric flow rate (Q_L) of 0.25 mL/min, followed by continuous flushing with CO-730-free water for 20 hours at the same value of Q_L. For the curve representing the kinetic model simulation, the parameters k_f, k_b, and b were obtained by LM parameter estimation. Values for these parameters are given in Table 5. The curves are plotted as a function of total column pore volumes (vt/L).

47
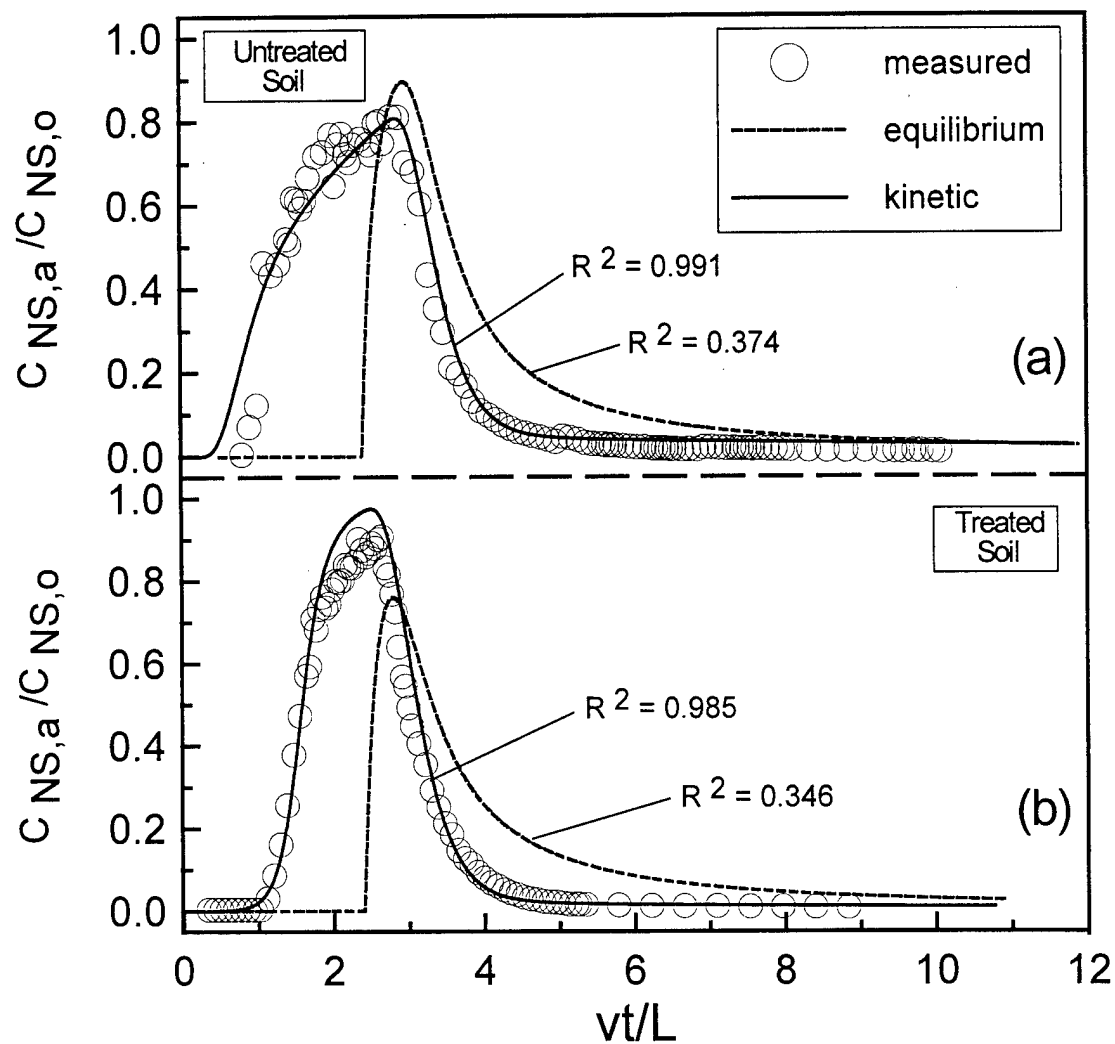
Figure 18. Measured and simulated (equilibrium and kinetic partitioning) CO-730 effluent breakthrough using: (a) untreated porous media, and (b) HDTMA-treated porous media.

48

Table 4. Simulation Parameters

Parameter	Simulations			
	A	B	C, D	E
HDTMA-Treated Aquifer Material	No	Yes	No (C); Yes (D)	Yes
Column cross-sectional area	$3.5\ cm^2$	$3.5\ cm^2$	$3.5\ cm^2$	$3.5\ cm^2$
Column length (L)	25 cm	25 cm	25 cm	25 cm
Porosity (θ)	0.35	0.40	0.46	0.46
Dry bulk density (ρ_b)	$1.65\ g/cm^3$	$1.66\ g/cm^3$	$1.52\ g/cm^3$	$1.52\ g/cm^3$
Longitudinal dispersivity (α_L)	2.22 cm	2.22 cm	2.22 cm	2.22 cm
Source condition	CO-730: Pulse TCB: N/A[a]	CO-730: Pulse TCB: N/A	CO-730: N/A TCB: Pulse	CO-730: Continuous TCB: Pulse
Source concentration	CO-730: 50 g/L TCB: N/A	CO-730: 50 g/L TCB: N/A	CO-730: N/A TCB: 16.44 mg/L	CO-730: 50 g/L TCB: 16.44 mg/L
Volumetric flow rate	0.25 mL/min	0.25 mL/min	0.25 mL/min	0.25 mL/min
Volume of source fluid added	CO-730: 75 mL TCB: N/A	CO-730: 75 mL TCB: N/A	CO-730: N/A TCB: 75 mL	CO-730: 6 L TCB: 75 mL
Average pore water velocity (v)	12.4 cm/hr	10.91 cm/hr	9.42 cm/hr	9.42 cm/hr

[a] Not Applicable

**Table 5. Kinetic Langmuir Parameters Used in
CO-730 Transport Simulations**

Soil Condition	b (mg/g)	k_f (mL/mg hr)	k_b (1/hr)	R^2
HDTMA-Treated	7.4	1.8×10^{-1}	1.8×10^{-2}	0.985
Untreated	9.2	9.0×10^{-3}	3.6×10^{-2}	0.983

In both Figures 18a and 18b the simulated breakthrough curves obtained using the equilibrium two-term Langmuir partitioning relationship do not adequately describe the measured data, suggesting that during these experiments local equilibrium was not attained. Previous researchers (31) have noted that failure to attain local equilibrium can depend on a number of factors (e.g., pore water velocity, dispersion coefficients, boundary conditions, form of partitioning relationship); in this case it is most likely a result of the relatively high pore water velocities used in our experiments. It should be noted, however, that the pore water velocities used in our experiments are well within the range of those observed at the Columbus, MS field site (15). Additionally, significant increases in near-field pore water velocities would be expected when surfactant remobilization is applied at a field site. Thus, the expectation of kinetic effects during nonionic surfactant enhanced remobilization is reasonable.

It is clear from Figures 18a and 18b that the kinetic model provides a reasonable fit to the measured data, whereas the equilibrium model does not; this is also illustrated by comparison of the R^2-values between the measured and simulated curves given in Table 5. However, because the kinetic simulations required indirect estimation of the parameter b and the mass transfer terms k_f and k_b, it is difficult to assess the overall validity of our choice for a kinetic partitioning relationship. Nevertheless, Figures 18a and 18b strongly indicate that kinetic effects dominated the transport process, and as employed Equation (22) adequately represents these effects.

Effluent breakthrough curves for simulations C and D (Table 4) are shown in Figures 19a and 19b, respectively. In these simulations a pulse of 16.44 mg/L TCB was input into the column for 5 hours, followed by continuous flushing with clean water for 20 hours (all at Q_L=0.25 mL/min). For simulation C, TCB transport was modeled through untreated porous media [K_d=1.49 mL/g; (7)]; for simulation D, TCB transport was modeled through HDTMA-treated porous media [K_d=43 mL/g; (47)]. Both simulations assumed physical porous media characteristics corresponding to measured values in a TCB remobilization experiment discussed in (47) and Section IV (simulation E). As these figures show, HDTMA-treated porous media is a much more favorable partitioning medium than untreated porous media. In the untreated porous media, the

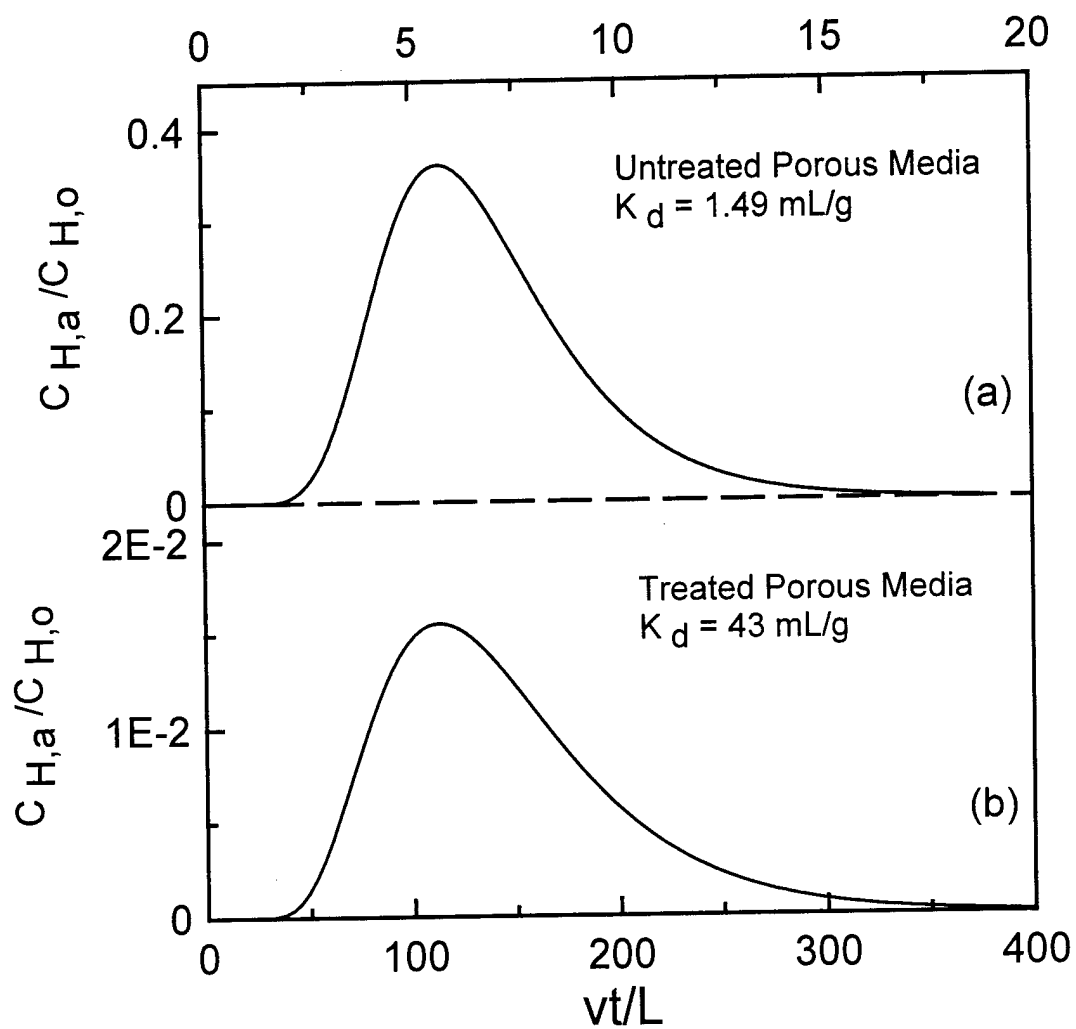**Figure 19.** Simulated TCB effluent breakthrough using: (a) untreated porous media, and (b) HDTMA-treated porous media.

initial TCB breakthrough begins after approximately 1.5 pore volumes have been eluted; in the HDTMA-treated porous media this occurs after approximately 35 pore volumes. This is consistent with expected results based on a simple comparison of the retardation coefficients ($R=1+(\rho_b/\theta)K_d$) for TCB in these media: $R_{untreated} \approx 6$, $R_{treated} \approx 142$, and $R_{treated}/R_{untreated} \approx 24$. Similarly, approximately 19 column pore volumes are required to elute essentially all of the TCB in the untreated porous media; in the HDTMA-treated porous media approximately 450 column pore volumes are required.

Coupled TCB and CO-730 transport representing simulation E (Table 4) is shown in Figure 20. Measured concentration data from an experiment discussed in (47) are also shown in this figure for comparison. In these simulations, a pulse of 16.44 mg/L TCB was input into the column for 5 hours, followed by flushing with clean water for 65 hours, and then flushing with water containing 50 g/L CO 730 for 30 hours (all at Q_L=0.25 mL/min). The curve representing CO-730 transport was obtained using the kinetic Langmuir model (Equation (22); b, k_f, and k_b for HDTMA-treated porous media [Table 5]), and appears to match the experimental data well. The difference in the plateau values (1.0 for the simulation verses ~0.95 for the experimental) is a measure of the error in the CO-730 analysis (~5%; (47)). For the TCB transport, two simulation curves are shown: in one, the value for $\kappa_{pm,NS}$ (0.59 g/mg) used was determined by LM parameter estimation using Equation (20) and the batch data described in (47); in the other, $\kappa_{pm,NS}$ (0.27 g/mg) was determined using LM parameter estimation and the dynamic model (Equations (20), (25)-(29)) described above. From these curves it is apparent that the value for $\kappa_{pm,NS}$ determined using the dynamic model provides a closer fit to the experimental data than does the $\kappa_{pm,NS}$ determined using the static (batch) approach, although the dynamic model overestimates the maximum TCB effluent concentration and underestimates the TCB concentration of the tailing portion of the curve. The exact reasons for this are unclear, although it is likely that the uncertainty associated with using a large number of experimental and empirical parameters in our model contributes to this effect. The sensitivity of the model to $\kappa_{pm,NS}$ suggests that treating this parameter as a constant may not be appropriate over the entire range of CO 730 concentrations. As noted by other researchers (39, 50), it is reasonable to expect that at low aqueous CO 730 concentrations, sorbed CO 730 (mostly as monomers) would not appreciably increase the TCB sorptive capacity of the solid phase; thus, $\kappa_{pm,NS}$ would be relatively small. As the aqueous CO 730 concentration exceeds the CMC, sorption of both monomers and micelles would likely increase the TCB sorptive capacity of the solid phase, increasing the value of $\kappa_{pm,NS}$.

Another possible explanation for the differences between the measured and simulated data in Figure 20 follows from the representation of TCB solubility in Equation (20). TCB partitioning into the monomer and micellar psuedophases is modeled as two distinctly different linear processes above and below the CMC, with the partitioning coefficients (K_{MN} and K_{MC} in Equation (20)) determined from the slopes of the linear portions of a plot of TCB solubility versus aqueous CO 730 concentration (47).
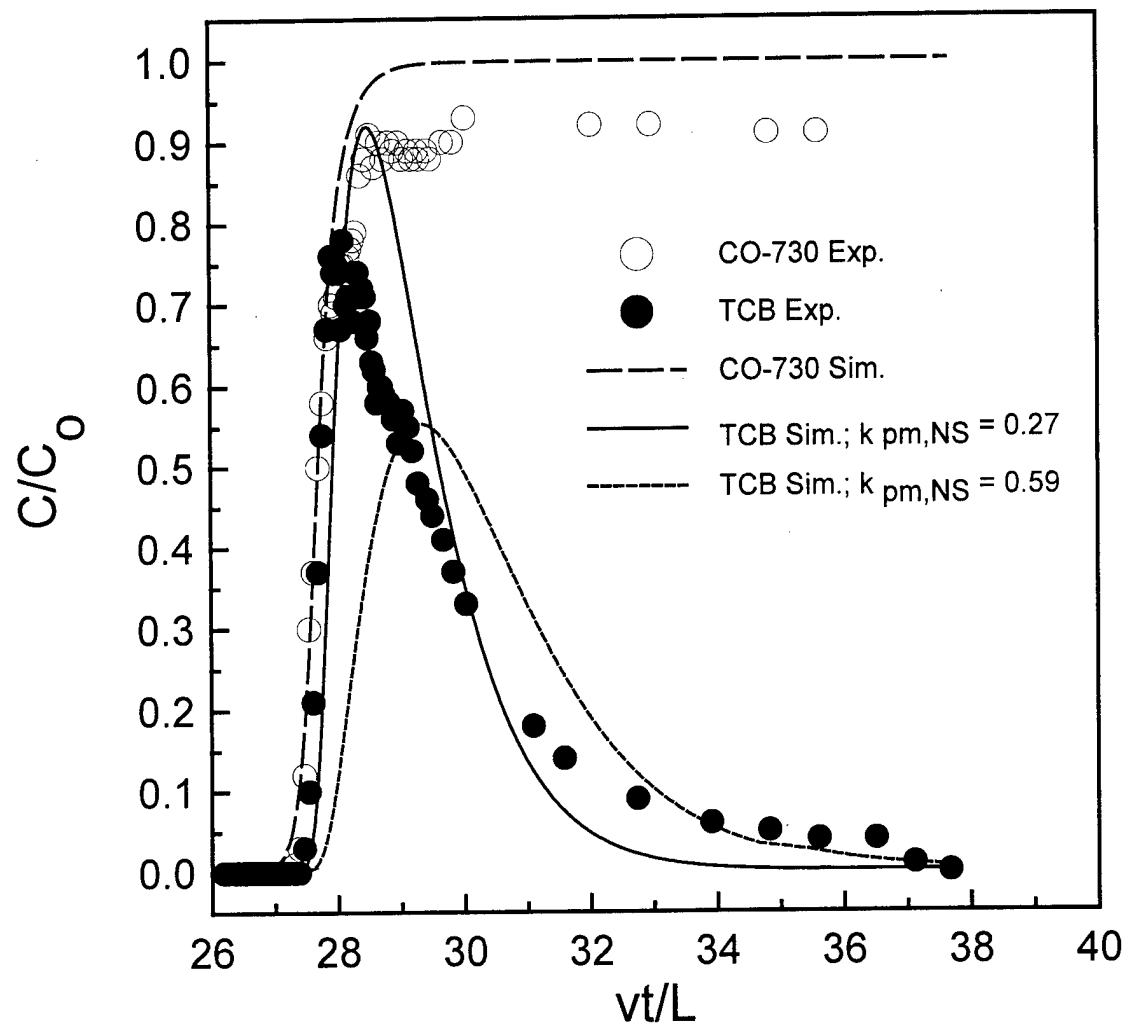
Figure 20. Measured and simulated CO-730 and TCB effluent breakthrough using HDTMA-treated porous media. Simulated CO-730 breakthrough obtained using kinetic Langmuir equation; simulated TCB breakthrough obtained for two different $\kappa_{pm,NS}$ values.

However, it is more likely that TCB solubility enhancement changes gradually near the CMC. In this regard, previous researchers (39) have defined a transitional partitioning coefficient to account for this effect. These researchers have applied this transitional model to batch data with good results, although this approach requires an additional fitting parameter. In the case of our dynamic model, it is questionable whether an additional fitting parameter is justified, considering the previously noted uncertainty in the measured and empirical parameters and the adequate representation of the experimental data by the model.

Sensitivity of the model to influent nonionic surfactant concentrations is shown in Figure 21. All simulations assumed physical porous media characteristics corresponding to simulation E (Table 4). To initiate a simulation, a 5 hour pulse of TCB (16.44 ppm) was introduced at the column inlet, at a constant volumetric flow rate (0.25 mL/min). This was followed by a constant input (0.25 mL/min) of aqueous CO-730 solution for the duration of the simulation. CO-730 concentrations were varied between 25 g/L and 100 g/L. Breakthrough curves for CO-730 at the column outlet are shown in Figure 21a. The shift to earlier breakthrough at higher influent CO-730 concentrations indicates a decrease in the apparent retardation of the surfactant. This is a result of the Langmuir-type rate-limited sorption isotherm: as influent surfactant concentrations increase, the mass fraction of sorbed surfactant decreases, thereby decreasing surfactant retardation. All of the breakthrough curves in Figure 21a are characterized by an abrupt initial rise, followed by a more gentle approach to a maximum value. This reduction in apparent dispersion is also a result of Langmuir-type sorption: the leading front of the surfactant solution is more strongly sorbed, resulting in a reduction in dispersion in the initial portion of the breakthrough curves. Similar trends in nonionic surfactant breakthrough curves have been noted in previous studies (51, 52).

In Figure 21b, TCB breakthrough curves corresponding to the respective influent surfactant concentrations are shown. TCB breakthrough occurs at earlier times and apparent dispersion of TCB decreases with increased influent surfactant concentrations, similar to CO-730 breakthrough behavior. Increased influent CO-730 concentrations result in a more rapid removal of TCB, requiring less flushing volume to achieve a given level of removal. Also, as influent CO-730 concentration increases, the effluent to influent TCB ratio ($C_{H,a}/C_{H,o}$) exceeds 1. This can be explained by a "concentrate and strip" mechanism: TCB is concentrated within the HDTMA-treated sorbent zone, but is stripped when CO-730 flushing occurs. At higher CO-730 concentrations there are more micelles available, therefore TCB partitioning into the micellar pseudophase is more efficient and the concentrating effect is more pronounced. A similar mechanism has been proposed (4) to explain effluent/influent ratios greater than 1 for aqueous dichlorobenzene eluting from a column packed with aquifer material treated with the cationic surfactant dodecylpyridinium.
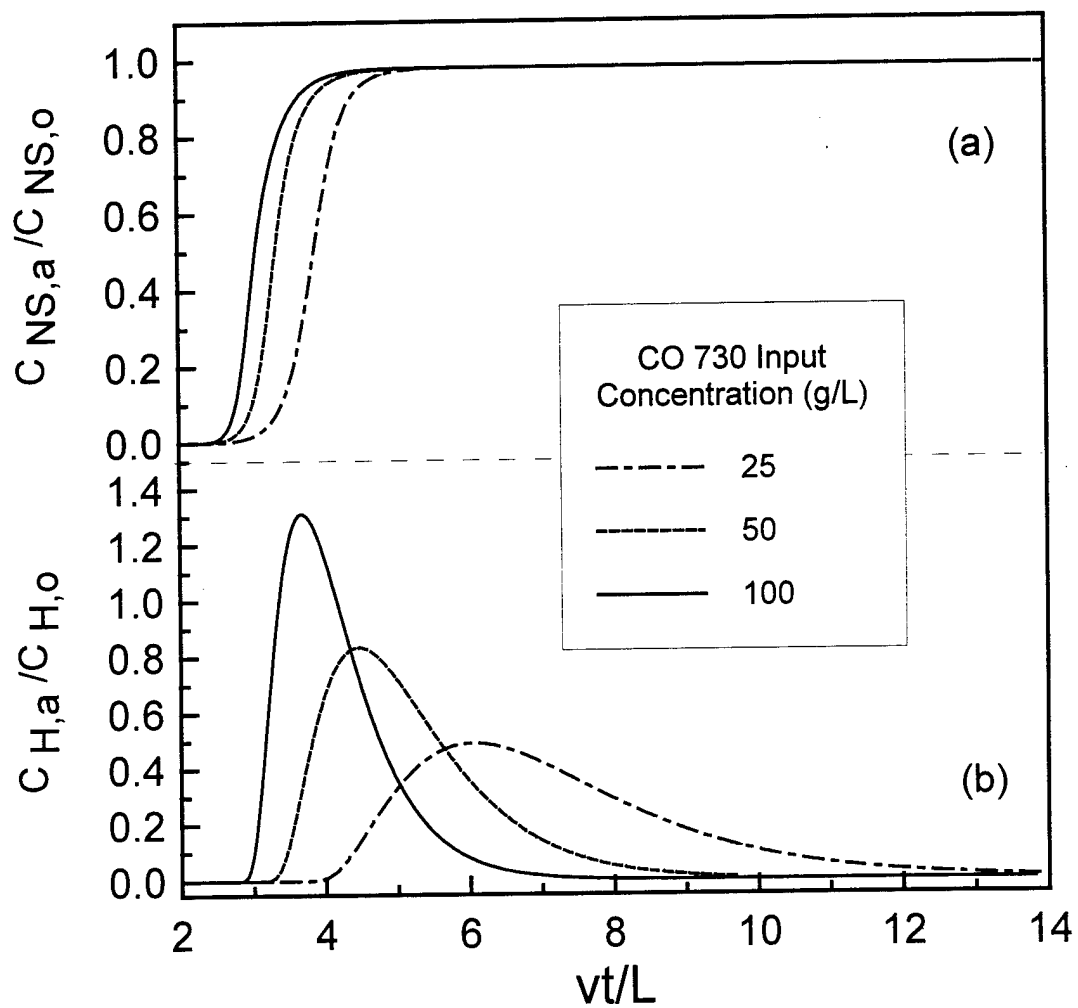
54

Figure 21. Effect of influent CO-730 concentration on (a) CO-730 and (b) TCB effluent breakthrough.

Simulations examining the model sensitivity to surfactant flushing rates were performed using physical porous media characteristics corresponding to simulation E (Table 4). To initiate a simulation, a 5 hour pulse of TCB (16.44 ppm) was introduced at the column inlet, at a constant volumetric flow rate (0.25 mL/min). This was followed by a continuous input of aqueous CO-730 solution (50 g/L) at a different (but constant) volumetric flow rate, for the duration of the simulation. Flushing rates were varied between 0.05 mL/min and 0.25 mL/min, corresponding to average pore water velocities between 1.9 cm/hr and 9.4 cm/hr. Breakthrough curves for CO-730 and TCB at the column outlet are shown in Figures 22a and 22b, respectively. For both CO-730 and TCB, breakthrough occurs at earlier times for higher flow rates. Also, the apparent CO-730 dispersion decreases as flushing rates increase, indicated by the more rapid rise and roll-off to the maximum value for increasing values of Q_L (Figure 22a). Both effects are the result of Langmuir-type sorption (Equation (29)) and an increase in advective transport relative to dispersive transport (Equation (23a)) at higher flow rates.

In Figure 22b, the normalized TCB concentration ($C_{H,a}/C_{H,o}$) is plotted as a function of time rather than the dimensionless parameter vt/L (which is a function of the CO-730 flushing rate). In Figure 23, $C_{H,a}/C_{H,o}$ is plotted as a function of the dimensionless CO-730 flushing volume, Q_F/V_p (Q_F [L_a^3] is the volume of CO-730 solution flushed, V_p [L_a^3] is the column pore volume). As this figure illustrates, the volume of CO-730 required to remove the sorbed TCB is independent of the flushing rate. This is a result of the equilibrium form of the TCB partitioning relationship (Equation (19)).

Based on Figures 21b and 23, it is tempting to conclude that the apparent dependence of TCB removal efficiency on surfactant concentration and flushing rates could be exploited when applying the enhanced sorption/enhanced solubilization remediation scheme in a field situation by flushing high concentration nonionic surfactant solutions at large pore water velocities through the enhanced sorbent zone. However, at abnormally high pore water velocities, mass transfer limitations in HOC partitioning may occur, invalidating the assumption of equilibrium partitioning used here (Equations (19) and (20)). In this regard, there is evidence (51) that mass transfer limitations would likely have a detrimental effect on HOC removal: larger volumes of aqueous nonionic surfactant solution would be required to achieve a given level of HOC removal at higher pore water velocities. Thus, it is likely that there is an ideal nonionic surfactant flushing rate which corresponds to the maximum flushing rate under which the equilibrium assumption for HOC/solid-phase partitioning is still valid. Flushing rates which exceed this ideal value will not produce added HOC removal efficiency. The limitations on influent aqueous nonionic surfactant concentrations are both physical and practical: at large aqueous concentrations, the unique properties of surfactants (foaming, etc.) make them difficult to work with. Also, increasing surfactant concentration corresponds to an increase in material costs, which may not be beneficial when compared to the increase in HOC removal efficiency. These considerations suggest that optimization of the enhanced sorption/enhanced
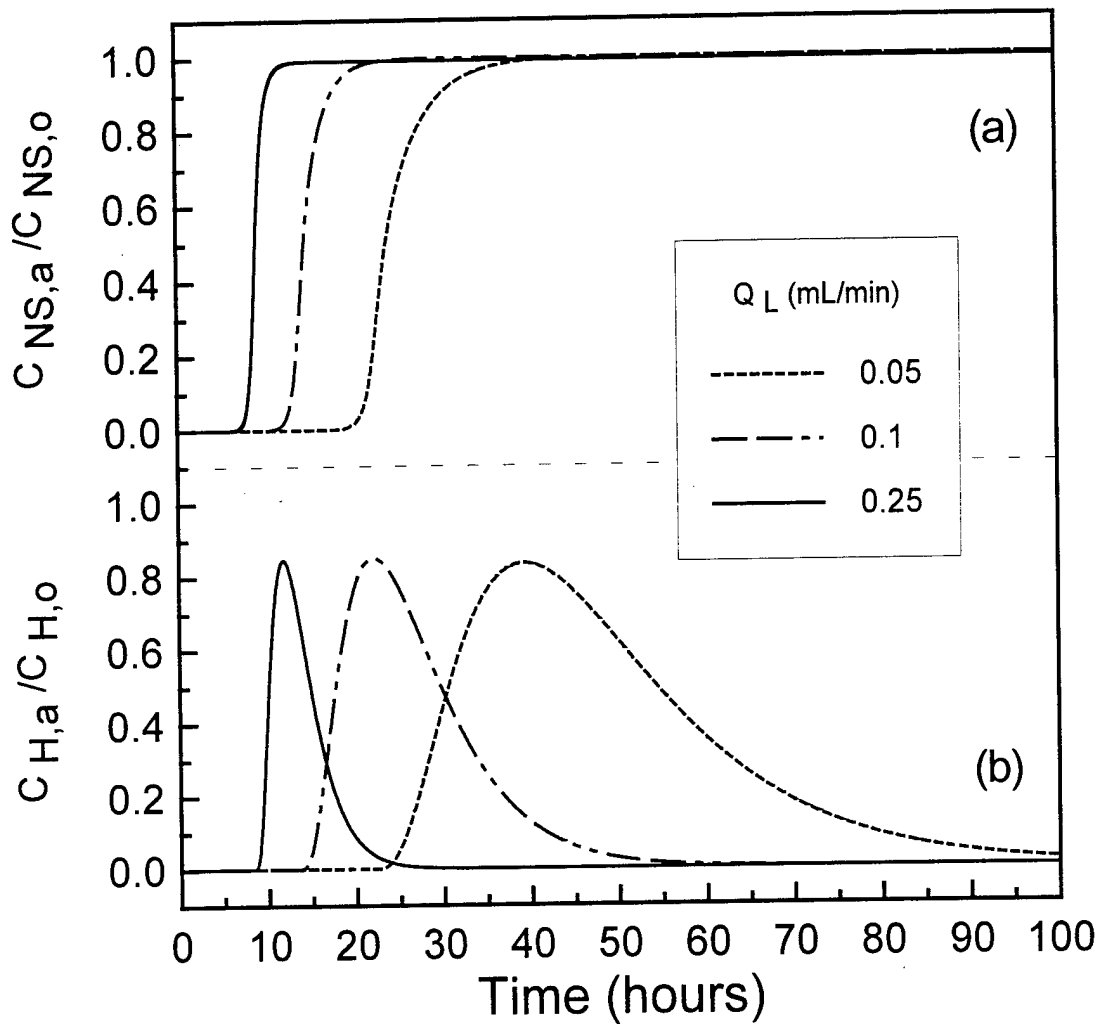
Figure 22. Effect of CO-730 flushing rate on (a) CO-730 and (b) TCB effluent breakthrough.
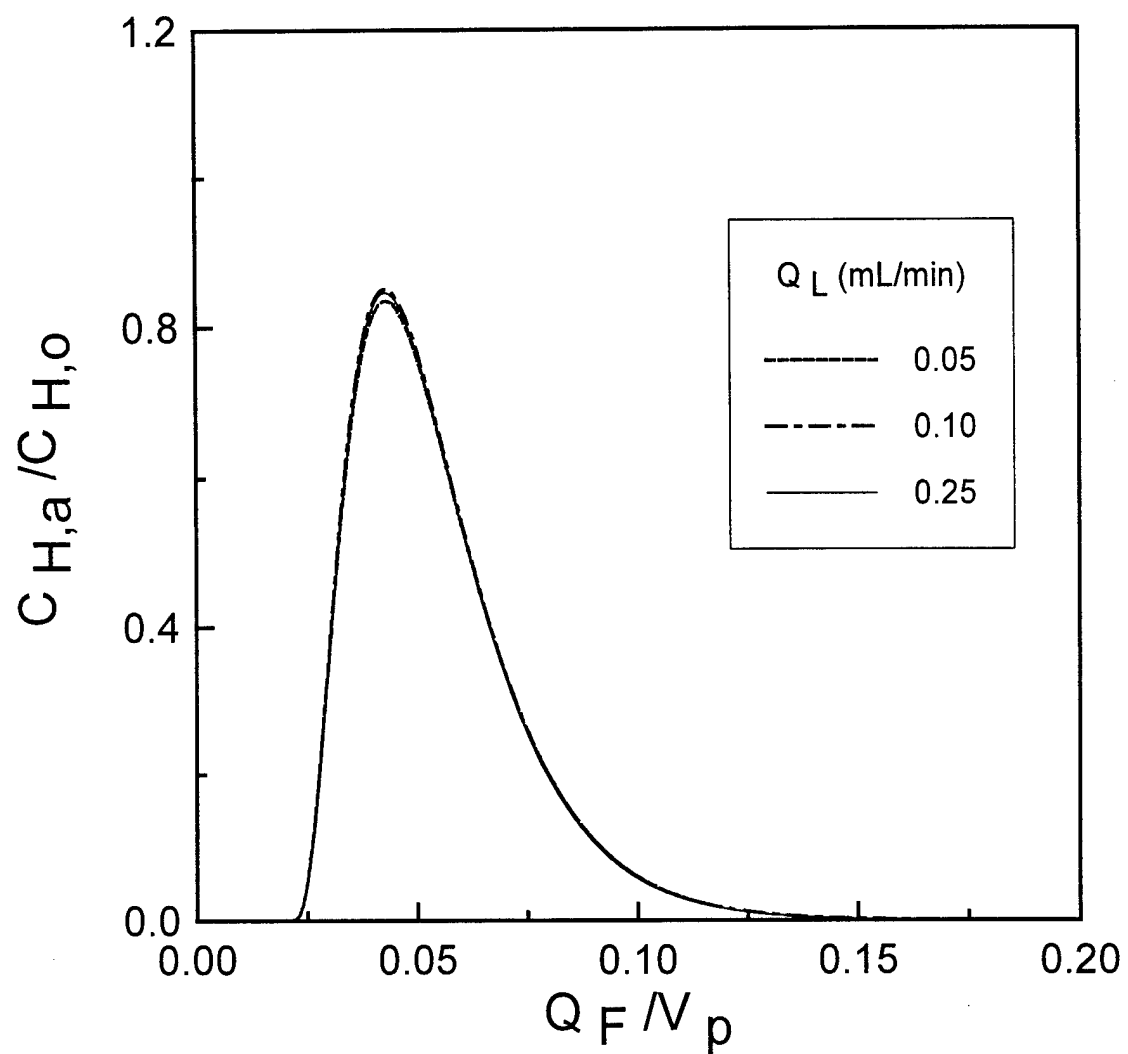
Figure 23. Simulated TCB effluent breakthrough as a function of CO-730 flushing volume and flushing rate.

solubilization remediation scheme at a field site will require, in addition to laboratory batch studies to determine partitioning relationships as described in *(47)* and in the previous sections of this report, laboratory experimentation coupled with numerical simulation to determine whether HOC/solid phase mass-transfer limitations will occur at the anticipated flow rate.

SECTION VI

CONCLUSIONS

The potential utility of an *in situ* enhanced sorbent zone created using cationic surfactants in the remediation of HOCs in groundwater is dependent upon a contaminant removal process. Nonionic surfactant-enhanced solubilization to remobilize an HOC entrapped within an enhanced sorbent zone (created using a cationic surfactant) has been shown to be a promising HOC removal process.

In situ emplaced sorbent zones were created in flow-through column and box model aquifer systems by the injection of aqueous solutions of a cationic surfactant (HDTMA) into those systems. The results suggest that significant reductions in hydraulic conductivity due to the surfactant injections did not occur. The results indicate that it is feasible to produce cationic surfactant-enhanced sorbent zones in situ within aquifers by underground injection.

Cationic surfactant simulation results indicate that the transport and partitioning of HDTMA in Columbus aquifer material are mass-transfer limited. The assumption that the primary mass-transfer limiting step was desorption, based in part on conclusions from previous studies, provided a reasonable fit to the experimental results. Kinetic partitioning, with desorption as the likely mass transfer-limiting step, is expected to dominate for Columbus aquifer material under both natural gradient flow, and induced flow conditions associated with development of an enhanced sorption zone.

This study is believed to be one of the first to describe the simulation of cationic surfactant transport where desorption, described by both a kinetic Langmuir and a kinetic modified BET partitioning relationship, is the limiting mass-transfer mechanism. Both of these partitioning relationships produced comparable results, which suggests that the kinetic Langmuir relationship should be used when modeling cationic surfactant transport, since it is the easier of the two relationships to incorporate into existing transport models.

Simulation results suggest that the difference between fast and slow sorption kinetics is of little importance, compared to desorption kinetics. Slow desorption kinetics can be expected to facilitate the *in situ* sorbent zone concept by: 1) slowing the overall mobility of the sorbent zone; and 2) lowering the background aqueous surfactant concentration within the zone. The lower background aqueous concentrations should minimize the toxic effects of the surfactant on microbial populations and subsequent biodegradation of organic contaminants.

The apparent CMC for the nonionic surfactant used, CO-730, was found to decrease significantly from ~10 g/L to ~0.6 g/L in the presence of 7 ppm HDTMA, a cationic surfactant. Low aqueous HDTMA concentrations are expected within a developed *in situ*

60

enhanced sorbent zone created using HDTMA. The apparent CO-730 CMC in the presence of HDTMA-modified Columbus aquifer material was also ~0.6 g/L, in agreement with the aquifer material-free system. The reduction in the apparent CMC observed is believed to be due to non-ideal mixed micelle formation. A greater portion of the nonionic surfactant will be present in the micellar pseudophase, which is the phase required for remobilization, as a result of the lowered CMC. This significant reduction in the apparent CMC is beneficial to the concept of remobilizing HOCs sorbed to modified aquifer material.

The partitioning behavior of TCB, the model HOC chosen for this study, in the HDTMA-modified aquifer material/water systems was found to depend on the aquifer material organic carbon content, the apparent CO-730 CMC, and the partitioning of TCB between the micellar pseudophase and the bulk aqueous phase containing surfactant monomers. The results of the batch sorption experiments conducted indicate that the micellar pseudophase is a more favorable partitioning medium for TCB relative to the solid phase organic carbon within an enhanced sorbent zone. The efficient removal of HOCs from a sorbent zone requires effective HOC partitioning into the mobile nonionic surfactant solution.

One-dimensional column experiments were performed in HDTMA-treated and untreated aquifer materials to determine the transport behavior of CO-730, and to assess the feasibility of using CO-730 to mobilize and recover TCB bound within a cationic surfactant-enhanced sorbent zone. Complete removal (> 99%) of the bound TCB was accomplished using a 12 column pore volume flush of 50 g/L CO-730. The results demonstrate that a nonionic surfactant can effectively remove a hydrophobic organic contaminant from an enhanced sorbent zone created using a cationic surfactant.

Simulations of CO-730 transport and partitioning experiments in columns containing HDTMA-treated and untreated Columbus AFB aquifer material were performed using both an equilibrium two-term Langmuir and a kinetic Langmuir partitioning relationship. The coefficients used in the equilibrium simulations were determined from batch experiments, while those used in the kinetic simulations were obtained by parameter estimation methods. These simulations demonstrated that rate-limited mass transfer of CO-730 had likely occurred during the experiments, and that the kinetic Langmuir relationship adequately described the partitioning behavior of CO-730.

Simulations of coupled CO-730/TCB transport and partitioning experiments in a column containing HDTMA-treated Columbus AFB aquifer material were performed using the kinetic Langmuir relationship to describe the partitioning behavior of CO-730. The forward and reverse mass-transfer coefficients utilized in the CO-730 transport model were obtained by calibrating the model to previously performed CO-730 transport experiments. With the exception of one parameter (the partitioning coefficient for TCB between sorbed CO-730 and the bulk solid phase, $\kappa_{pm,NS}$), all of the coefficients in the TCB partitioning relationship were determined from batch experiments. Values for $\kappa_{pm,NS}$ were determined

by fitting batch data to the apparent TCB soil-water distribution expression (providing a "static" $\kappa_{pm,NS}$), and by fitting column data to the coupled CO-730/TCB model (providing a "dynamic" $\kappa_{pm,NS}$). Simulations show that the best agreement between the experimental and simulated CO-730 and TCB breakthrough curves is achieved using the dynamic $\kappa_{pm,NS}$.

Sensitivity analysis of the system containing HDTMA-treated soil, CO-730, and TCB illustrated the potential effects of surfactant influent concentrations and surfactant flushing rates on HOC recovery from within cationic surfactant-enhanced sorption zones. The analysis revealed that increasing CO-730 influent concentrations decreased the volume of surfactant solution required to recover a given pulse of TCB. The likely mechanism for this is a "concentrate and strip" phenomenon which occurs when TCB concentrated within an HDTMA-treated enhanced sorbent zone is solubilized by a flushing CO-730 solution. The concentrating effect is enhanced at higher CO-730 influent concentrations because more micelles are available, therefore TCB partitioning into the micellar pseudophase is more efficient. The analysis also revealed that TCB removal increased as CO-730 flushing rates increased, although a maximum flow rate likely exists which corresponds to the rate at which mass-transfer limitations in the TCB/solid phase partitioning become apparent. This analysis illustrates the need to consider the potential for mass-transfer limitations for both the flushing nonionic surfactant and the HOC when designing enhanced sorption/enhanced solubilization remediation applications.

The focus of the study described in this report has been on understanding the transport and partitioning behavior of a cationic surfactant in natural aquifer materials, and on understanding the dynamic partitioning behavior of an HOC in a cationic surfactant-enhanced sorption zone undergoing remobilization via nonionic surfactant solubilization. Batch and column experiments and numerical simulations indicate that this enhanced sorption/enhanced solubilization method has potential as a technique for remediating groundwater contaminated with dissolved organic contaminants.

Based on the results of this study, it is possible to speculate on the types of field sites at which surfactant-enhanced sorption/surfactant-enhanced solubilization may be useful for remediating HOCs in groundwater. Near surface, relatively homogeneous unconsolidated aquifers in which the HOC plume has a relatively small areal distribution are potential candidates for this remediation method. The aquifer material should have a porosity in the range of 30-40%, a CEC >2.0 meq/100g, and a low natural organic carbon content (<0.1% OC). Aquifer hydraulic conditions should be such that a bulk average horizontal pore water velocity of approximately 0.2 m/day can be sustained over the time period required to develop the cationic surfactant sorbent zone, and during periodic flushing of the sorbent zone with nonionic surfactants to solubilize and recover sorbed HOCs.

SECTION VII

RECOMMENDATIONS

Further research investigating this promising remediation strategy is warranted. In particular, laboratory-scale multidimensional physical modeling should be performed to address questions of preferential surfactant distributions in mildly heterogeneous systems.

Research into surface treatment methods for separating and recovering the nonionic surfactant from the extracted effluent stream is required. Without such recovery methods, it is unlikely that this remediation technique will prove cost effective.

An economic analysis of the remediation method should be performed, comparing the method to other established plume remediation techniques (e.g., pump-and-treat) for a hypothetical field site. If such an analysis indicates that the method is cost-effective, then a field-scale demonstration of the method would be appropriate.

SECTION VIII

REFERENCES

(1) Mackay, D. M.; Cherry, J. A. Groundwater contamination: Pump-and-treat remediation. *Environ. Sci. Technol.* **1989**, 23, 6, 630-636.

(2) Burris, D. R.; Cherry, J. A. Emerging plume management technologies: *In situ* treatment zones. In: *Proceedings of the 8th Annual Meeting of the Air and Waste Management Association*, Kansas City, MO., **1992**; 92-34.04.

(3) Burris, D. R.; Antworth, C. P. *In situ* modification of an aquifer material by a cationic surfactant to enhance retardation of organic contaminants. *J. Contam. Hydrol.* **1992**, 25, 325-337.

(4) Wagner, J.; Chen, H.; Brownawell, B. J.; Westall, J. C. Use of cationic surfactants to modify soil surfaces to promote sorption and retard migration of hydrophobic organic compounds. *Environ. Sci. Technol.* 1994, 28, 231-237.

(5) Hayworth, J. S.; Burris, D. R. Modeling cationic surfactant transport in porous media. *Ground Water.* **1996**, 34, 2, 274-282.

(6) Boyd, S. A.; Jaynes, W. F.; Ross, B. S. Immobilization of organic contaminants by organo-clays: Application to soil restoration and hazardous waste containment. In *Organic Substances and Sediments in Water. Volume 1, Humics and Soils*; Baker, R. A., Ed.; Lewis Publishers: Chelsea, Michigan, **1991**; 181-200.

(7) Brown, M. J. *Enhancement of Organic Contaminant Retardation by the Modification of Aquifer Material with Cationic Surfactants*; M. S. Thesis, Univ. of Waterloo, Waterloo, Ontario, Canada, **1993**.

(8) Burris, D. R.; Antworth, C. P. Potential for subsurface *in situ* sorbent systems. *Groundwater Manage.* **1990**, 4, 527-537.

(9) Ventullo, R. M.; Larson, R. J. Adaptation of aquatic microbial communities to quaternary ammonium compounds. *Applied and Environ. Microbiol.* **1986**, 51, 356-361.

(10) Nye, J. V.; Guerin, W. F.; Boyd, S. A. Heterotrophic activity of microorganisms in soils treated with quaternary ammonium compounds. *Environ. Sci. Technol.* **1994**, 28, 944-951.

(11) Crocker, F. H.; Guerin, W. F.; Boyd, S. A. Bioavailability of naphthalene sorbed to cationic surfactant-modified smectite clay. *Environ. Sci. Technol.* **1995**, 29, 2953-2958.

(12) Kile, D. E.; Chiou, C. T. Water solubility enhancements of DDT and trichlorobenzene by some surfactants below and above the critical micelle concentration. *Environ. Sci. Technol.* **1989**, 23, 832-838.

(13) Edwards, D. A.; Liu, Z.; Luthy, R. G. Surfactant solubilization of organic compounds in soil/aqueous systems. *J. Environ. Eng.* **1994**, 120, 1, 23-41.

(14) Chiou, C. T.; Porter, P. E.; Schmedding, D. W. Partition equilibria of nonionic organic compounds between soil organic matter and water. *Environ. Sci. Technol.* **1983**, 17, 227-231.

(15) Boggs, J. M.; Beard, L. M.; Waldrop, W. R.; Stauffer, T. B.; Macintyre, W. G.; Antworth, C. P. Transport of tritium and four organic compounds during a natural gradient experiment (MADE-2). *Electric Power Research Institute*, RP-2485-05, **1993**.

(16) Burris, D. R.; Antworth, C. P.; Stauffer, T. B.; MacIntyre, W. G. Humic acid-modified silica as a model aquifer material. *Environ. Toxicol. Chem.* **1991**, 10, 433-440.

(17) MacIntyre, W. G.; Stauffer, T. B.; Antworth, C. P. A comparison of sorption coefficients determined by batch, column, and box methods. *Ground Water.* **1991**, 29, 908-913.

(18) Bear, J. *Hydraulics of Groundwater*, McGraw-Hill, New York, 1991.

(19) Sposito, G. *The Surface Chemistry of Soils*. Oxford Univ. Press, New York, 1984.

(20) Fetter, C. W. *Contaminant Hydrogeology*, Macmillan Publishing Co.: New York, **1993**.

(21) Tamamushi, B.; Tamaki, K. *Proc. Intern. Congr. Surface Activity, 2nd. London.* 3, 449, **1957**.

(22) Brunauer, S.; Emmett, P. H.; Teller, E. Adsorption of gases in multimolecular layers. *J. Am. Chem. Soc.* **1938**, 60, 309-319.

(23) Huyakorn, P. S.; Pinder, G. F. *Computational Methods in Subsurface Flow*, Academic Press, Inc.; New York, **1983**.

(24) van Genuchten, M. Th.; Parker, J. C. Boundary conditions for displacement experiments through short laboratory soil columns. *Soil Sci. Soc. Am. J.* **1984**, 48, 703-708.

(25) Goode, D. J.; Konikow, L. F. Modification of a method-of-characteristics solute-transport model to incorporate decay and equilibrium-controlled sorption or ion-exchange. *U.S. Geol. Survey. Water-Res. Invest. Rep. 89-4030,* **1989**.

(26) Marquardt, D. W. An algorithm for least-squares estimation of nonlinear parameters. *J. Soc. Indust. Appl. Math.* **1963**, 11, 431-441.

(27) Brownawell, B. J.; Chen, H.; Collier, J. M.; Westall, J. C. Adsorption of organic cations to natural materials. *Environ. Sci. Technol.* **1990**, 24, pp. 1234-1241.

(28) Xu, S.; Boyd, S. A. Cationic surfactant sorption to a vermiculitic subsoil via hydrophobic bonding. *Environ. Sci. Technol.,* **In Review**.

(29) Anacker, E. W. Micelle formation of cationic surfactants in aqueous media. In *Cationic Surfactants*; Jungermann, E., Ed.; Marcel Dekker, Inc.: New York, **1970**; 203-288.

(30) Valocchi, A. J. Validity of the local equilibrium assumption for modeling sorbing solute transport through homogeneous soils. *Water Resour. Res.* **1985**, 21, 6, 808-820.

(31) Bahr, J. B.; Rubin, J. Direct comparison of kinetic and local equilibrium formulations for solute transport affected by surface reactions. *Water Resourc. Res.* **1987**, 23, 3, 438-452.

(32) Biyani, P.; Goochee, C. F. Nonlinear fixed-bed sorption when mass transfer and sorption are controlling. *AIChiE J.* **1988**, 34, 10, 1747-1751.

(33) Bales, R. C.; Szecsody, J. E. Microscale processes in porous media. In: *Chemical Modeling of Aqueous Systems II,* D. C. Melchior, D. C.; Bassett, R. L., ed., American Chemical Society Symposium Series 416, **1990**.

(34) Nye, J. V.; Guerin, W. F.; Boyd, S. A. Heterotrophic activity of microorganisms in soils treated with quaternary ammonium compounds. *Environ. Sci. Technol.* **1994**, 28, 944-951.

(35) Ventullo, R. M.; Larson, R. J. Adaptation of aquatic microbial communities to quaternary ammonium compounds. *Applied and Environ. Microbiol.* **1986**, 51, 2, 356-361.

(36) Gregg, S. J.; Sing, K. S. *Adsorption, Surface Area, and Porosity*. Academic Press, Inc., New York, 1982.

(37) Ruthven, D. M. *Principles of Adsorption and Adsorption Processes*. John Wiley & Sons, New York, **1984**.

(38) Sun, S.; Inskeep, W. P.; Boyd, S. A. Sorption of nonionic organic compounds in soil-water systems containing a micelle-forming surfactant. *Environ. Sci. Technol.* **1995**, 29, 903-913.

(39) Hayworth, J. S.; Burris, D. R. Nonionic surfactant-enhanced solubilization and recovery of organic contaminants from within cationic surfactant-enhanced sorbent zones. 1. Experiments. *Environ. Sci. Technol.* **In Review** (1).

(40) Burris, D. R.; MacIntyre, W. G. Water solubility behavior of binary hydrocarbon mixtures. *Environ. Toxicol. Chem.* **1985**, 4, 371-377.

(41) Adamson, A. W. *Physical Chemistry of Surfaces*; John Wiley & Sons, New York, **1982**.

(42) Sposito, G. On the use of the Langmuir equation in the interpretation of "adsorption" phenomena: II. The "two-surface" Langmuir equation. *Soil Sci. Soc. Am. J.*, **1982**, 46, 1147-1152.

(43) Scamehorn, J. F.; Harwell, J. H. Precipitation of surfactant mixtures. In *Mixed Surfactant Systems*; Ogino, K.; Masahiko, A., Eds.; Marcel Dekker, Inc.: New York, **1993**; 283-315.

(44) Shiau, B.; Harwell, J. H.; Scamehorn, J. F. Precipitation of mixtures of anionic and cationic surfactants. III. Effect of added nonionic surfactant. *J. Colliod Interface Sci.* **1994**, 167, 332-345.

(45) Hayworth, J. S.; Burris, D. R. Nonionic surfactant-enhanced solubilization and recovery of organic contaminants from within cationic surfactant-enhanced sorbent zones. 2. Numerical simulations. *Environ. Sci. Technol.* **In Review** (2).

(46) Adeel, Z.; Luthy, R. G. Sorption and transport kinetics of a nonionic surfactant through an aquifer sediment. *Environ. Sci. Technol.* **1995**, 29, 1032-1042.

(47) Travis, C. C.; Etnier, E. L. A survey of sorption relationships for reactive solutes in soil. *J. Environ. Qual.* **1981**, 10, 1, 8-17.

(48) Gu, T.; Zhu, B.-Y; Rupprecht, H. Surfactant adsorption and surface micellization. *Progr. Colloid Polym. Sci.* **1992**, 88, 74-85.

(49) Abriola, L. M.; Dekker, T. J.; Pennell, K. D. Surfactant-enhanced solubilization of residual dodecane in soil columns. 2. Mathematical modeling. *Environ. Sci. Technol.* **1993**, 27, 2341-2351.

(50) Abdul, A. S.; Gibson, T. L. Laboratory studies of surfactant-enhanced washing of polychlorinated biphenyl from sandy material. *Environ. Sci. Technol.* **1991**, 25, 665-671.